[Journal of the Faculty of Science, Hokkaido University, Ser. VII (Geophysics), Vol. V, No. 3, 1978]

Lateral Variation of the Upper Mantle Structure around Northern Japan and its Application to Hypocenter Determination

Sadaomi SUZUKI

(Received May 29, 1978)

Abstract

Travel times of seven shallow earthquakes with redetermined hypocentral parameters are analysed to reveal the areal distribution of *P*-wave velocity in the upper mantle beneath the Japanese islands and their margin. The areal distribution of *P*-wave velocity is derived from the *P*-wave travel time residuals different for the regions which are characterized by the arrivals being early in the eastern half of the Japanese arc and being late in the western half of the Japanese arc.

Analysis of travel times of the 1973 Nemuro-Oki earthquake and its aftershocks shows that a *P*-wave velocity in the uppermost part of the mantle beneath the Pacific coastal area between the Japan trench and the Aseismic Front is 8.1 km/sec and increases from that value as a depth increases; the velocity increase to a depth of about 100 km in the upper mantle is slightly lower than that obtained from the J-B tables. The travel time residuals in Hokkaido for the earthquakes near the Kanto region give that the *P*-wave velocity of the upper mantle below the trench is larger than that below the Pacific coast. In addition to these velocities, the *Pn* velocity beneath the northern region in the Honshu island is also obtained to be 7.59 km/sec, using the travel times of the 1970 Southeastern Akita and the 1974 Izu-Hanto eathquake. Through the analyses, the inference that the *Pn* velocity under the volcanic region might be lower than the average *Pn* velocity beneath the whole region of the island was not confirmed.

The lateral variation of the upper mantle structure shown in terms of the areal distribution of *P*-wave velocity demonstrates that the epicenters of the 1973 Nemuro-Oki earthquake and its aftershocks located by USGS differ systematically from these located by the regional network of JMA. Assuming a simple three dimensional mantle structure, we obtained epicenter solutions of main and aftershocks of large earthquakes of $M=6.7$ or larger in and around Hokkaido.

The 1973 Nemuro-Oki earthquake had the initial rupture located at a depth 36 km with being accompanied by many aftershocks, most hypocenters of which were determined to be shallower than the depth of the main shock. The rupture of the earthquake started from the uppermost part of the mantle on the coastal side and came up to just under the sea bottom near the trench.

1. Introduction

1.1 *Introduction*

The Japanese islands and their vicinity are located in the most active regions in the world. In the Pacific Ocean between the Japanese islands and the Japan trench, a number of great earthquakes occur and seismicity in both shallow and intermediate depths is extremely high. To understand the characteristics of occurrence of great earthquake as well as features of high seismicity, accurate hypocenter determination is always required. In earthquake prediction, the hypocentral determination is also required, because the previous detection of seismic gaps and change in seismic velocities which signals the coming of an earthquake strongly depends on the accurate hypocentral determination.

For the earthquakes occurring off the Pacific coast, however, it is most likely that the hypocenters we determined deviate systematically from the actual ones[1),2)]. These biased hypocentral locations may result not only from the fact that we have no observing stations with ocean bottom seismographs in the Pacific coast area, but also from the fact that the Japanese island arc has anomalous crust and upper mantle structures.

The purpose of the present paper is to investigate more closely the anomalous crust and upper mantle structures especially beneath the northern half of Japan to which the existence of the seismic active zone should be related. The investigation includes showing the anomalous crust and upper mantle structures as areal distributions of *P*-wave velocities in which the rate of increase in velcoties with depth, that is, the velocity gradient in upper mantle is to be noted as well.

For the upper mantle below the Japanese island arc, a number of studies have shown that a lateral variation of seismic velocities exists (e.g., UTSU[1)]); the seismic velocities in the upper mantle beneath the Pacific trench and its inner margin are considerably higher than those beneath the Japanese islands. A regional variation in *Pn* velocity under the Honshu island has been also derived by the recent explosion-seismic studies. The derived regional variation is that a low *Pn* velocity of 7.53 km/sec exists beneath the northeastern part of Honshu and a high *Pn* velocity of 8.1 km/sec, beneath the northeastern region between the Pacific coast and the Japan trench (ASANO et al.[3)]; OKADA et al.[4)]). A boundary at which change in the *Pn* velocity occurs is inferred to be almost coincident with the "Asesimic Front" proposed by YOSHII[5)] (SUZUKI[6)]; OKADA et al.[4)]).

On the basis of the previously obtained lateral variation of seismic velocities in the upper mantle, the area to be considered is divided into five regions of A to E as shown in Fig. 1, which are tentatively bounded by the trench axis, the Aseismic Front, the Volcanic Front and the coast-line of the Sea of Japan.

Since *Pn* phase can be recorded as first arrival at station with an epicentral distance less than 1100 km, the upper mantle structure shallower than a depth of about 100 km will be investigated.

1.2 *Data*

Locations of seismographic stations used for travel time analysis are

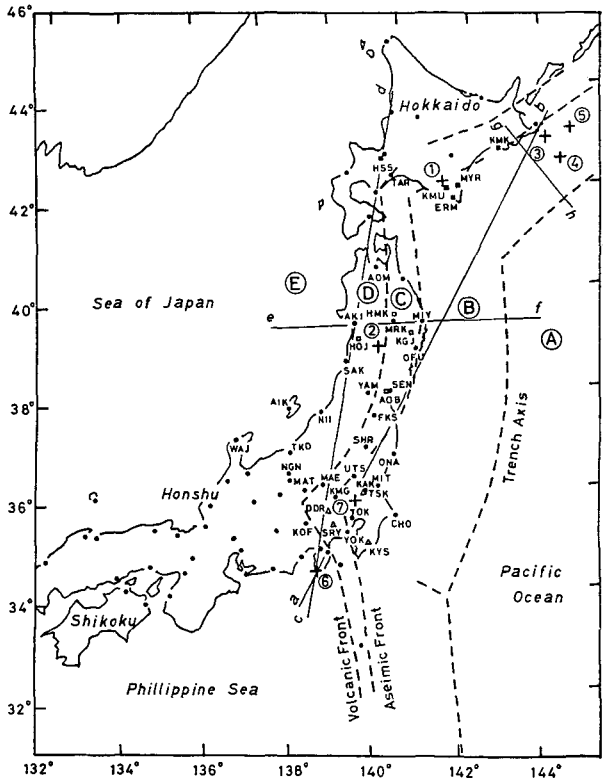

Fig. 1 Map showing the region to be discussed. The solid circles, solid squares, open squares, and open triangles represent the seismometric stations of JMA, Hokkaido University, Tohoku University, and University of Tokyo, respectively. Numbers attached to the earthquake epicenters refer to index numbers listed in Table 1. A~E are the regions bounded by the three tectonic lines (broken lines) and the coast of the Sea of Japan.

Table 1. Earthquake Data

No.	Data	Date and Time (GMT)	Origin Time	Epicenter		Depth	M
		d h	m s	°N	°E	km	
1	Relocation[29]	1970 Jan. 20 17	33 04.1	42.40	143.13	53	
	JMA		33 03.8	42.38	143.13	50	6.7
	USCGS		33 05.4	42.5	143.0	46	6.3
2	Relocation[30]	1970 Oct. 16 05	26 12.3	39.20	140.74	6	
	JMA		26 09.8	39.20	140.75	0	6.2
	USCGS		26 13.3	39.3	140.7	24	5.8
3	Relocation[6]	1973 Jun. 17 03	55 04.3	43.09	145.83	36	
	JMA		55 01.8	42.97	145.95	40	7.4
	NOAA		55 02.9	43.2	145.8	48	7.7*
4	Relocation[6]	1973 Jun. 17 20	37 56.7	42.65	146.19	35	
	JMA		37 54.6	42.48	146.08	40	6.1
	NOAA		37 57.3	42.7	146.0	50	6.0*
5	Relocation[6]	1973 Jun. 24 02	43 24.0	43.19	146.67	35	
	JMA		43 21.9	42.95	146.75	30	7.1
	NOAA		43 25.9	43.3	146.4	50	7.1*
6	Relocation[31]	1973 May 08 23	33 27.9	34.67	138.80	11	
	JMA		33 27.3	34.57	138.80	10	6.9
	USGS		33 25.2	34.5	138.7	2	6.5*
7	Relocation**	1974 Aug. 03 18	16 34.0	36.08	139.91	62	
	JMA		16 34.7	36.02	139.92	50	5.8
	USGS		16 34.0	36.0	139.8	58	5.6
8	Relocation**	1973 Sep. 30 06	17 52.4	35.71	140.69	55	
	JMA		17 52.0	35.65	140.67	50	5.9
	USGS		17 52.8	35.6	140.4	62	5.9
9	JMA	1973 Oct. 01 14	16 20.8	35.62	140.8	60	5.8
	USGS		16 23.0	35.7	140.6	56	5.6
10	JMA	1973 Dec. 26 20	30 06.1	33.57	140.92	40	5.5
	USGS		30 06.4	33.4	140.8	63	5.6
11	JMA	1974 Mar. 03 04	50 47.8	35.57	140.88	60	6.1
	USGS		50 48.9	35.6	140.6	46	5.6
12	JMA	1974 Jul. 08 05	45 37.8	36.42	141.20	40	6.3
	USGS		45 37.0	36.4	141.1	35	6.0
13	JMA	1974 Sep. 27 03	10 06.2	33.61	141.52	60	6.4
	USGS		10 07.9	33.6	141.1	46	5.8
14	JMA	1974 Nov. 15 23	32 41.1	35.75	141.25	40	6.1
	USGS		32 42.1	35.8	141.0	36	5.8
15	JMA	1975 Jan. 20 17	31 08.7	34.98	141.35	30	5.9
	USGS		31 10.6	35.0	141.2	28	5.9

*: M_S **: after TSUMURA (personal letter)

shown in Fig. 1. Most of the stations are those of the Japan Meteorological Agency (JAM). The other stations in which high sensitive seismographs are installed are those of three universities, Hokkaido University, Tohoku University, and University of Tokyo. From travel times at these stations, apparent P-wave velocities of the upper mantle are to be determined. In the analysis, data of first arrivals of P-waves were selected in which onset of the first arrival is identified as iP or P so that the error of first arrival time may be less than 0.2 sec. The earthquake parameters used for the analysis are given in Table 1, their epicenters being shown in Fig. 1 and Fig. 8 with the attached numbers which correspond to those for the earthquakes in Table 1. Data sets used for determining locations of aftershocks are different in earthquakes. Most of the stations used for the earthquakes before 1969 are those of JAM while the stations used for the earthquakes after 1970, those of JMA and Hokkaido University.

2. Lateral variation of P-wave velocity in the upper mantle

2.1 Areal distribution of travel time residuals

The areal distribution of travel time residuals is shown in Fig. 2 in which Fig. 2a and 2b show the travel time residuals for the two earthquakes that occurred in Hokkaido, and Fig. 2c and 2d, those for the other two earthquakes that occurred in Kanto. These travel time residuals are due to the anomalous crust and upper mantle structures in which the spatial distributions of P-wave velocities are different.

The travel time residuals in Fig. 2a and 2b were obtained from the 1973 Nemuro-Oki and the 1970 Hidaka earthquake, respectively. These travel time residuals are negative values at most stations. However, in the travel time residuals at stations in the northern part of Hokkaido and near the coast of the Sea of Japan, the following features are included: 1) in Hokkaido, the stations located more north have larger positive values of residuals, 2) in Honshu, a negative correlation between travel time residual and length of seismic ray traveling in the seismic area under the Pacific Ocean exists, and 3) in the Tohoku region, the stations located more east have smaller values of residuals.

The travel time residuals in Fig. 2c and 2d were obtained from the 1974 Izu-Hanto and the 1974 Ibaragi earthquake in Kanto, respectively. These travel time residuals have the following features: 1) the arrivals at stations near the ocenaic coast are earlier than those at stations near the coast of the Sea of Japan, and 2) the remarkable difference in the residuals from 6 to 7

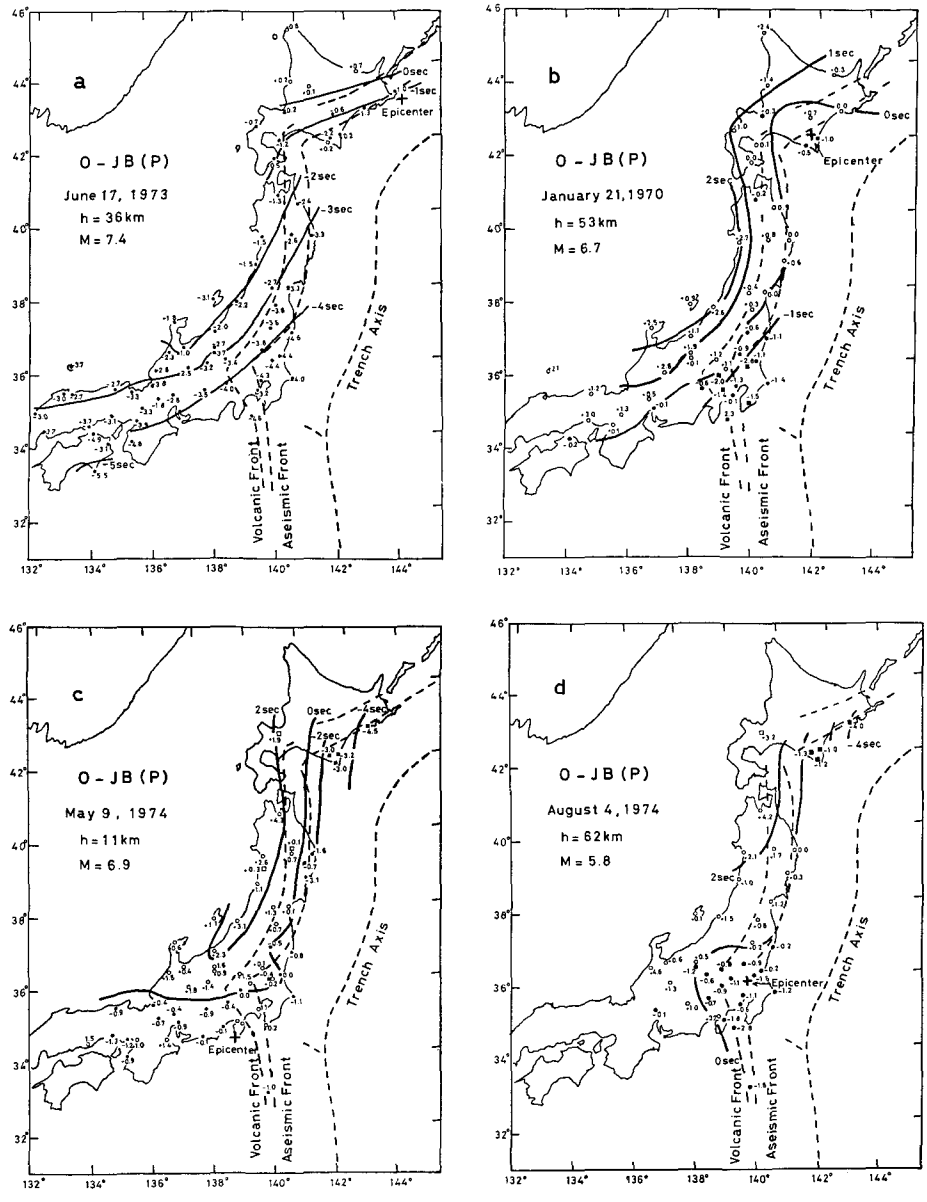

Fig. 2 *P* travel-time residuals (in seconds) relative to the Jeffreys-Bullen table. The solid circles are the stations having negative residuals and the open circles are the stations having positive residuals.

sec exists between KMK in the eastern part of Hokkaido and HSS in the western part of Hokkaido.

Among these features, a thing common to the travel time residuals for the four earthquakes is that the stations near the Pacific coast have the negative values of residuals approximately proportional to the lengths of ray paths of seismic waves traveling under the Pacific Ocean. Travel time residuals in the Kanto region for the Nemuro-Oki earthquake are about −4 sec which is much the same as those in the eastern Hokkaido region for the Izu-Hanto or the Ibaragi earthquake. On the other hand, for the Hidaka earthquake, travel time residuals in Kanto region are about −1 sec, which is however almost the same as that at station KMU for the Ibaragi earthquake. The difference in both travel time residuals may be caused by the fact that the *P*-wave velocities of the upper mantle near the trench are larger than that near the Aseismic Front under the Pacific Ocean.

2.2 Travel time curves and models of the upper mantle structures

The object in this section is to obtain models of the upper mantle structures beneath northern Japan. From the areal distributions of travel time residuals, two different upper mantle structures can be derived: One is a structure with relatively high velocity beneath the region (region B) between the trench and the Aseismic Front, and the other, a structure with relatively low velocity beneath the regions (regions A and B) on the land side of the Aseismic Front.

i) Model of the upper mantle structure beneath region B

Travel time plots of first arrivals for the three shocks of the 1973 Nemuro-Oki earthquake series are shown in Fig. 3a. *Pn* phase is observed even at epicentral distances beyond 10°.

The travel times observed at stations in Honshu are smaller by 5 sec on the average than the J-B (Jeffreys and Bullen) or I-M (Ichikawa and Mochizuki[32]) travel times, while the travel times at stations on the oceanic side (solid symbols) are smaller by 1 sec on the average than the Herrin travel times. The travel times at only stations to which seismic waves travel the oceanic region by more than 80% of the epicentral distance are replotted in the upper part of Fig. 3a. For the interpretation of these observed travel-time plots, the four models, *A* through *D*, of the velocity structure with high *Pn* velocity were assumed (Fig. 4). Among these models, model *B* is to be selected as a better model because a travel time curve from which this model is inverted well fits

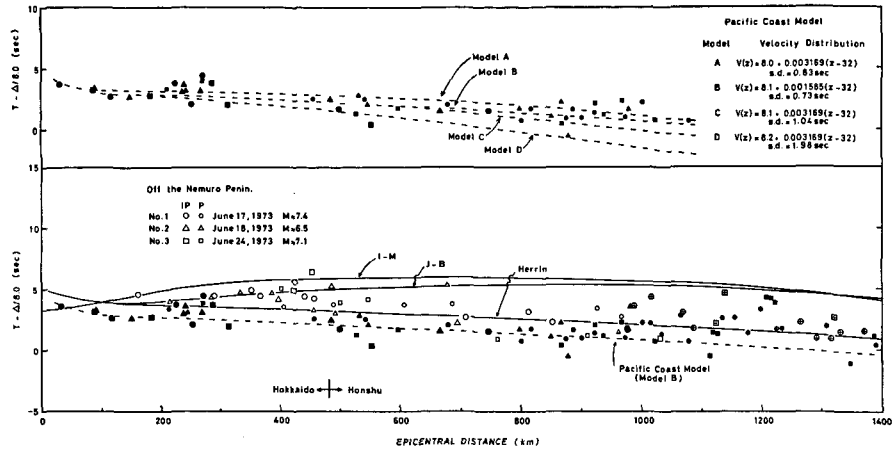

Fig. 3a

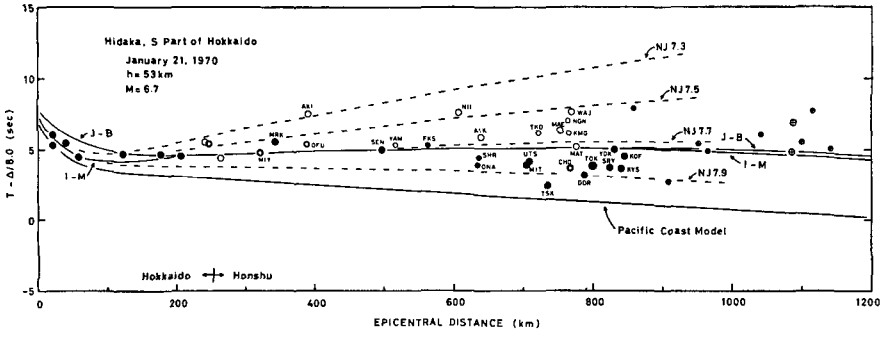

Fig. 3b

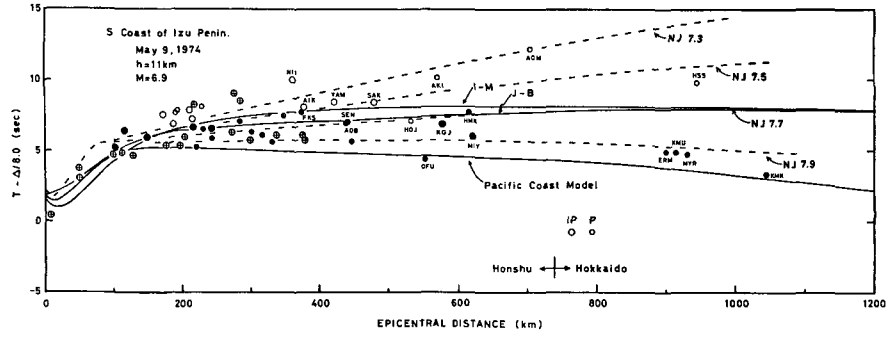

Fig. 3c

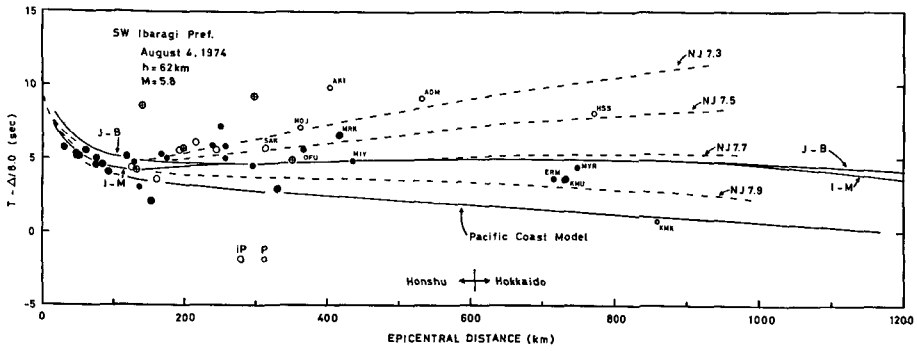

Fig. 3d

Fig. 3 Reduced travel-time diagrams for the six earthquakes listed in Table 1. The solid and open symbols represent the stations located on the oceanic side and the continental side of the Volcanic Front, respectively. The symbols with crosses represent the stations in the southwestern region of Japan. The dashed and solid curves represent the travel-time curves for the models of velocity distributions shown in Figure 4 and Figure 5, respectively.

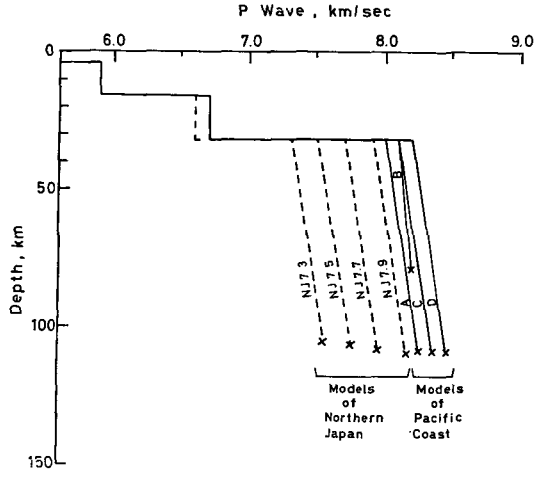

Fig. 4 Velocity distributions for the models of northern Japan and the models of the Pacific coast. The crosses represent the depths of penetration calculated for an epicentral distance of 1000 km when a focal depth of 10 km for the models of northern Japan and a focal depth of 40 km for the models of the Pacific coast are given.

the observed travel times. This model has a high *Pn* velocity of 8.1 km/sec and a velocity gradient with depth being more gentle than that estimated from the J-B travel time tables. Such gentle velocity gradient is also suggested

by UTSU[7] and YAMAMIZU[8]. When a lateral variation in velocity in the upper mantle exists, three dimensional propagation of seismic waves should be considered in general. If this consideration is made, a velocity gradient with depth to be derived from the travel time plots in the upper part of Fig. 3a may be still more gentle than that of model *B*.

In Fig. 5, we assume the Pacific Coast model as a crust and upper mantle structure beneath region B. This model is essentially the same as model *B* in depths shallower than 80 km, while that in depth deeper than 80 km is the same as the Mizoue-Tsujiura model[9].

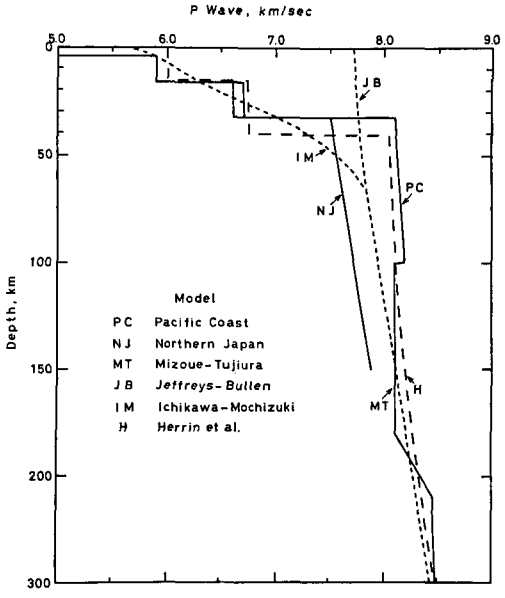

Fig. 5 *P*-wave velocity distributions for the Pacific Coast model, the Northern Japan model and others.

ii) Model of the upper mantle structure beneath regions C and D

Travel time plots of first arrivals for the three earthquakes, the 1970 Hidaka, the 1974 Izu-Hanto, and the 1974 Ibaragi earthquake are shown in Fig. 3b, 3c, and 3d respectively, in which a large scatter of travel time plots is observed. A greater part of the scatter may be caused by the regionality of crust and upper mantle structures. From these travel times, a velocity distribution beneath both regions C and D is to be obtained. In obtaining the velocity distribution, it must be assumed that the *Pn* velocity

under the island of the northern Japan arc is lower than that of the Pacific Coast model.

Figure 4 shows the four Northern Japan models as well as the Pacific Coast model. The velocity gradient in the upper mantle of the Northern Japan models is the same as that estimated from the *J-B* tables, and the *Pn* velocity is in a range of 7.3 to 7.9 km/sec. The travel time curves for these models are shown in Fig. 3b, 3c, and 3d, in which apparent *Pn* velocities beneath regions C and D are also in a range 7.3 to 7.9 km/sec.

2.3 Pn interval velocities

If a travel time correction for the regionality of crustal structure is applied to observed travel time, that is, the Moho time term is subtracted from the observed travel time, *Pn* interval velocity between focus and station site can be basically derived from the corrected travel time[4].

Data available for deriving the *Pn* interval velocity are selected among the data having such qualities as first arrival being due to earthquake with depth above or close to the Moho interface and as clear onset of the first arrival being recorded by high sensitive seismometer.

The travel time of *Pn* waves traveling in the uppermost part of the mantle for the earthquake having focus above the Moho interface is defined by

$$T = \Delta/V + \tau_s + \tau_0 \tag{1}$$

where T=travel time, Δ=epicentral distance, V=interval velocity, τ_s=Moho time term of focus, and τ_0=Moho time term at station, from which the *Pn* interval velocity can be derived, if Moho time terms at both station and focus are given. The required time terms were calculated from the empirical equation obtained by OKADA et al.[4] between the Moho time term and the Bouguer anomaly at a point:

$$\tau = 3.32 - 0.0063\,\Delta g \tag{2}$$

where τ is the Moho time term in second and Δg, the Bouguer gravity anomaly in milligal.

Figure 6 shows the *Pn* interval velocities obtained for the earthquakes 2, 3, and 6, which are also given in Table 2. In this figure, we observe that the *Pn* interval velocities along paths under the Pacific Ocean are higher than those under the Honshu island; the *Pn* interval velocities between the epicenter of earthquake 6 and stations KMK and HSS are 8.03 mk/sec and 7.66 km/sec, so that the difference between these velocities is about 7%.

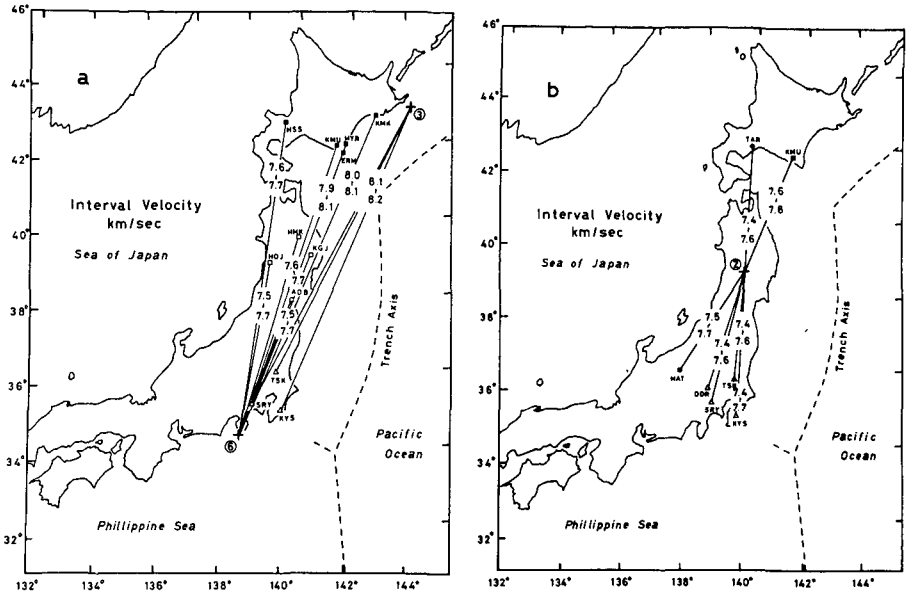

Fig. 6 Interval velocities in the upper mantle between the epicenters and the station sites. These values are tabulated also in Table 2.

The average value of the *Pn* interval velocities from the epicenter of earthquake 3 to stations TSK, SRY, and KYS is 8.14 km/sec which is higher by 6% than the *Pn* interval velocity from the epicenter of earthquake 6 to station HSS.

Figure 7 shows the seismic ray trajectories projected on the vertical sections along the *a-b* and *c-d* lines in Fig. 1. Shaded areas in the figure represent the seismic zones identifies with the hypocentral data of JMA. The greater part of the path from the origin of earthquake 6 to station HSS passes through the aseismic area, while the path from the origin of earthquake 6 to station KMK, as well as that from the origin of earthquake 3 to station TSK, passes through the seismic area.

For the ray paths beneath the island, regions C and D, there is little difference between the *Pn* interval velocities. The four ray paths shown in Fig. 6a from the origin of earthquake 6 to stations HOJ, AOB, KGJ, and HMK which pass through zones in the uppermost mantle beneath region D, region C or a region around the Volcanic Front. The *Pn* interval velocities obtained for these paths, are almost the same value, 7.6 to 7.7 km/sec. The five ray paths shown in Fig. 6b from the origin of earthquake 2 to stations

Table 2. Travel times and interval velocities of P waves for the three earthquakes in Table 1

Earthquake No.	Station	Moho Time-Term (sec)	Epicentral Distance (km)	Travel Time** (sec)	Interval Velocity (km/sec)
2 (1.9)*	KMU	3.2±0.1	386.3	55.5±0.5	7.66±0.10
	TAR	3.0±0.2	391.9	57.0±0.5	7.52±0.12
	TSK	2.4±0.4	336.4	49.3±0.3	7.48±0.12
	DDR	2.9±0.2	380.7	55.5±0.7	7.51±0.13
	SRY	3.1±0.1	419.2	60.7±0.8	7.52±0.12
	KYS	2.8±0.2	447.3	63.9±0.7	7.55±0.12
	MAT	3.4±0.1	370.0	53.7±0.5	7.64±0.10
3 (0.0)*	TSK	2.4±0.4	907.4	113.3±0.7	8.18±0.07
	SRY	3.1±0.1	1003.9	125.7±0.7	8.19±0.06
	KYS	2.8±0.2	1003.9	127.9±0.7	8.04±0.06
6 (1.7)*	KMK	2.2±0.5	1045.3	134.0±0.7	8.03±0.07
	MYR	3.1±0.1	932.0	121.3±0.8	8.00±0.06
	ERM	3.3±0.1	900.2	117.5±0.7	8.00±0.06
	KMU	3.2±0.1	915.6	119.3±0.8	8.00±0.06
	HSS	3.0±0.2	945.0	128.0±0.7	7.66±0.06
	HMK	2.7±0.3	614.5	84.5±0.7	7.67±0.10
	KGJ	2.6±0.3	578.8	79.2±0.7	7.72±0.11
	HOJ	2.9±0.2	532.7	74.3±0.7	7.63±0.10
	AOB	2.6±0.3	437.8	61.7±0.7	7.62±0.14

* Moho time-term at hypocenter, (sec).

** The fluctuation in the travel time is represented by the errors of observation and origin-time.

MAT, TSK, DDR, SRY, and TAR which pass also through zones in the uppermost mantle beneath region D, region C, or a region around the Volcanic Front. The *Pn* interval velocities obtained for these paths are almost the same value, 7.6 to 7.7km/sec as well. Thus, little difference in these *Pn* velocities seems to support the inference that the uppermost mantle beneath the island of the northern Japanese arc is of homogeneity, in which P wave velocity is in a range from 7.5 to 7.7 km/sec, the average being 7.59 km/sec.

The *Pn* interval velocity from the origin of earthquake 2 to station KMU is 7.66 km/sec, while that to station TAR is 7.52 km/sec. The difference between these *Pn* interval velocities, 0.14 km/sec, will produce a travel time difference of 1 sec when the *Pn* wave is propagated to a distance of 386.3 km. On the other hand, the *Pn* interval velocity from the origin of earthquake 6 to stations KMU, EMR, and MYR is 8.00 km/sec, while that to station HSS is 7.66 km/sec. The difference between these *Pn* interval velocities, 0.34 km/

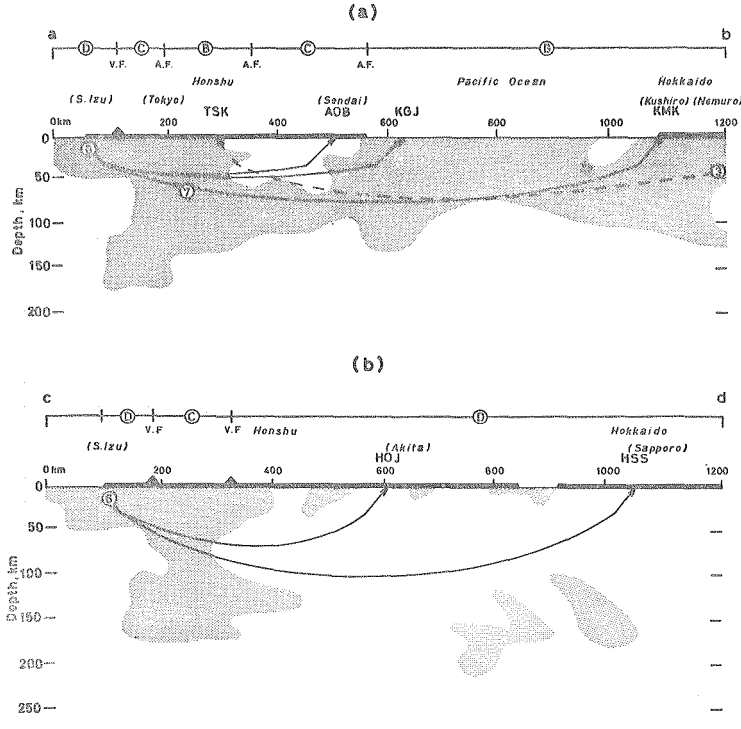

Fig. 7 (a) Ray paths projected on the vertical section along the *a-b* line shown in Figure 1. (b) Ray paths projected on the vertical section along the *c-d* line shown in Figure 1. Ray trajectories in (a) and (b) are calculated for the Pacific Coast model and the Northern Japan model shown in Figure 5, respectively. The shaded area represents the seismic zone identified with the hypocentral data of JMA. V.F. and A.F. indicate the Volcanic Front and the Aseismic Front, respectively. The regions of B, C, and D correspond to those defined in Figure 1.

sec, will produce a travel time difference of 4.5 sec when the *Pn* wave is propagated to a distance of about 900 km. Although the two ray paths from the earthquakes 2 and 6 to station KMU pass through much the same zone under region B, the effect of region B on the travel times for both paths quite different. The main cause of this difference may be on the fact that the least time path from the earthquake 6 to station KMU is strongly curved to the direction of the trench.

2.4 *Lateral variation of the upper mantle velocity under the Pacific coast*

In the sections 2.1 to 2.3, a lateral variation of the upper mantle velocity is derived under the Pacific coast (region B). In this section, the latteral variation of the upper mantle velocity is to be confirmed again in the travel time data for earthquakes occurring near Kanto region.

There are many observing stations in and around the Kanto region, so that hypocenters of earthquakes occurring near the Kanto region may be determined with high accuracy. Figure 8 shows the location map of the earthquakes and stations used for travel time analysis as well as the ray

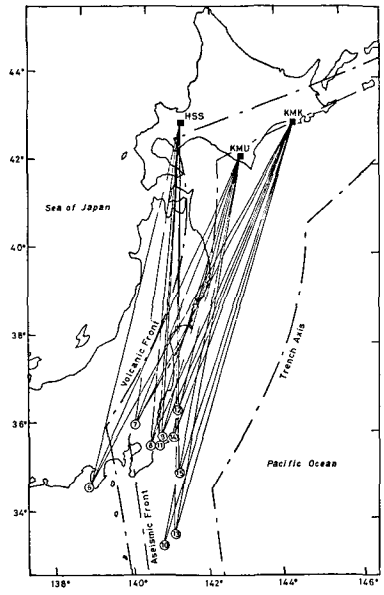

Fig. 8 Location map of the earthquakes and the stations used for travel time analysis.

paths for these earthquakes, the *O-C* times and epicentral distances for these earthquakes being given in Table 3. Earthquake data which were determined by the U.S. Geological Survey (USGS) are shown in Table 1. As seen in Table 3, negative values of *O-C* times for most paths are obtained at stations, HSS, KMU, and KMK. The average of the *O-C* times are –2.3 sec, –3.8 sec, and –5.8 sec, at stations HSS, KMU, and KMK, respectively. These average values show that the station located more east has the earlier arrival time; the *O-C* times almost depend on the location of station. However, the

Table 3. Residual travel times of P-waves

Earthquake No.	HSS			KMU			KMK		
	Δ (km)	O-C (sec)	L (km)	Δ (km)	O-C (sec)	L (km)	Δ (km)	O-C (sec)	L (km)
6	945.0	1.9	319	915.6	−3.0	249	1045.3	−4.5	213
7	772.5	3.2	286	732.6	−1.3	244	859.6	−4.0	190
8	807.0	−2.5	266	751.3	−3.2	196	869.5	−6.5	157
9	808.4	−3.9	260	754.2	−4.8	185	873.3	−6.5	151
10	1062.3	−5.9	218	999.3	−5.8	140	1109.2	−7.4	104
11	819.4	−1.7	263	764.9	−2.9	90	883.6	−4.9	132
12	728.9	−1.5	241	667.9	−2.0	179	784.6	−3.9	148
13	1039.5	−5.6	202	972.7	−6.8	126	1080.4	−7.8	90
14	795.7	−2.3	249	737.7	−3.2	174	850.1	−5.3	90
15	884.2	−4.4	224	818.1	−5.1	151	928.6	−6.7	109

discrepancies in the average values of O-C times are attributed not to the Moho time terms at these stations, but to the fact that there is a lateral variation in the upper mantle velocity under the Pacific coast, because difference between the Moho time terms at these stations may be 1 sec or less at most.

To measure a distance to what degree a ray path approaches the trench axis, let us define a mean value of distances, L, which is referred to as the mean distance, from the trench axis to the ray path

$$L = \frac{1}{\Delta}\int_0^{\Delta} l\,d\Delta \tag{3}$$

where l is a distance from a point on the ray path to the trench axis. The epicentral distances, Δ, and the mean distances for the earthquakes considered are given in Table 3. In Fig. 9 travel time residuals for the ray paths are plotted against the mean distances. Between the travel time residuals and the mean distances a fairly good correlation exists. The correlation coefficient between both quantities is 0.78. We assume that the relation between the travel time residual, δt, and the mean distance, L, can be expressed by the equation:

$$\delta t = a + bL + c\Delta \tag{4}$$

where a, b, and c are constants.

If the equation (4) is applied to the data for 28 ray paths except the two paths giving the positive values of residuals and the constants, a, b, and c are determined by the least square method, the relation between the travel time residuals and the mean distances is obtained as follows:

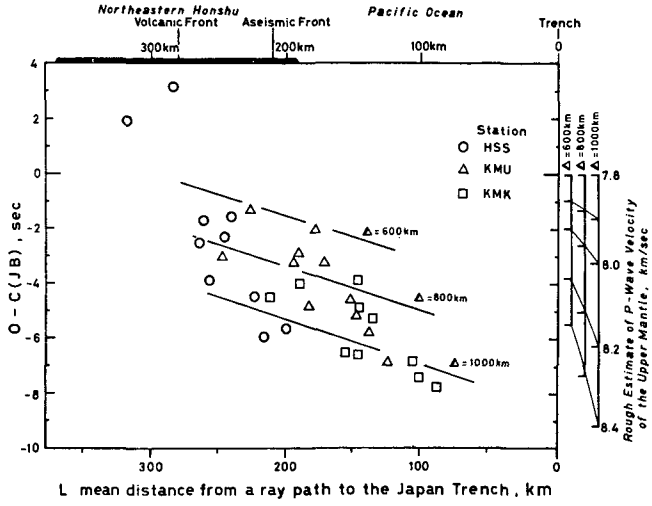

Fig. 9 Travel time residual obtained for each ray path plotted against the mean distance L from a ray path to the trench axis.

$$\delta t = (1.01\pm1.08) + (1.59\pm0.22)\times10^{-2}L - (9.56\pm0.97)\times10^{-3}\Delta \tag{5}$$

where δt is measured in seconds, and L and Δ, in kilometers.

On the other hand, travel time residual from focus A to a station B is, generally, represented by

$$\delta t = \int_A^B \frac{dS}{V} - \int_A^B \frac{dS'}{V_{JB}} \tag{6}$$

where S and V denote the actual ray path and the actual velocity, and S' and V_{JB}, the ray path and the velocity expected from the J-B tables.

Equation (6) is rewritten approximately by

$$\delta t \approx \frac{\Delta}{V} - \frac{\Delta}{V_{JB}} \tag{7}$$

(e.g., FEDOTOV and SLAVINA[10]).

Substituting (4) into (7) and considering $\delta t \cdot V/\Delta \ll 1$, we obtain

$$V(L) = V_{JB}^2\left(\frac{1}{V_{JB}} - c - \frac{a}{\Delta}\right) - \frac{bV_{JB}^2}{\Delta}L \tag{8}$$

This equation shows that the velocity in the uppermost mantle under the region from northeast Honshu to the Japan trench is proportional to the mean distance when epicentral distance is taken as parameter. Since $a=1.01$, $b=1.59\times10^{-2}$, and $c=-9.65\times10^{-3}$ in equation (5), and taking V_{JB} as 7.8 km/sec on the average velocity shallower than a depth of 80 km, then equation (8) when $\Delta=1000$ km is given by

$$V(L)=8.32-9.67\times10^{-4}L \tag{9}$$

Variations of $V(L)$ with the mean distance are shown in Fig. 9 when $\Delta=600$, 800, and 1000 km, in which scale for the velocity is shown on the right side of Fig. 9 for each epicentral distance.

The model B in Fig. 4 gives a bottom depth of about 80 km for ray paths with epicentral distances from 600 to 1000 km. This shows that the velocity as expressed equation (9) is taken as the average velocity in the upper mantle shallower than a depth of 80 km. This average velocity gradually increases from 8.0 km/sec under the coastal side to 8.3 km/sec under the Japan trench. The gradual increase in the velocity could be interpreted by assuming a high velocity layer with a dipping surface beneath region B. This high velocity layer could interpret an apparent velocity of about 8.5 km/sec obtained under the Pacific Ocean few tens kilometers east of the Japan trench[4] and also the existence of layer with 8.6 km/sec at a depth 60 to 80 km in the western Pacific Basin[11].

2.5 Laterally curved ray path

Within the region under which the velocity laterally increases depending on the empirical equation (9), a portion of waves will be propagated along such a path as being deviated from the great circle path; that is, the ray paths in this region are not such ones as illustrated in Fig. 8 by straight lines, but those curved toward the trench.

In Fig. 10, let us consider such a simplified case that Aseismic Front and trench axis are parallel to each other and in the region between these velocity changes as $V=V_0+kd$ in which no depth change in velocity is assumed, where d is a distance from the Aseismic Front, V a velocity at the distance d, V_0 a velocity at the Aseismic Front, and k a constant. The distance of the largest lateral deviation, $d_{\max}$, of the ray path from focus A to station B may be given by

$$d_{\max}=\frac{V_0}{k}\left(\sqrt{1+\left(\frac{k\Delta}{2V_0}\right)^2}-1\right) \tag{10}$$

When Δ=1000 km, V_0=8.0 km/sec, and k=9.67 $\times 10^{-4}$/sec according to equation (9), we obtained d_{max}=15 km.

Since both the trench axis and the Aseismic Front are practically not straight lines but curved ones as shown in Fig. 1, the actual ray paths may be more strongly curved than the ray path calculated by equation (10). Then, the mean distances in Fig. 9 might slightly be shifted to the right-hand side in plotting.

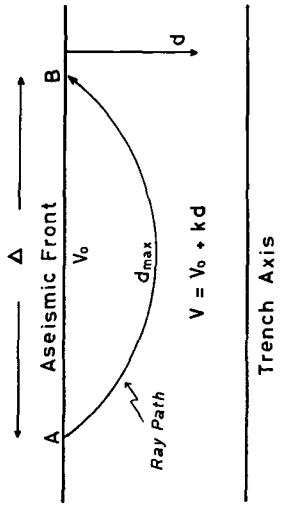

Fig. 10 Schematic representation of ray path for lateral increase of velocity.

3. Determination of earthquake hypocenters in taking into account the lateral variation of the upper mantle velocity under northern Japan

3.1 A method for locating earthquake hypocenters

In this section, a new method of hypocenter determination for earthquakes occurring under the Pacific coastal areas will be introduced. Since the upper mantle under the Japanese island arc has the complicated structures obtained in the previous chapter, seismic data at distant stations are unfavorable for precise hypocenter determination; therefore data of stations at epicentral distances less than hundreds of kilometers should be used.

To develop the method, the following assumptions are made: (1) The crust and upper mantle structure is one shown in Fig. 11, in which the uppermost mantle consists of two regions bounded by the Aseismic Front; the region on the landside has a velocity of 7.5 km/sec and that on the Oceanic side, a velocity of 8.1 km/sec. The crustal structure is assumed by referring to the structure of DEN et al.[12], which has a Moho time term of 3.28 sec if Pn=8.1 km/sec, or of 2.86 sec if Pn=7.5 km/sec. (2) A value of V_p/V_s is assumed to be 1.77 that is the same as the average of V_p/V_s values in the Hokkaido and Tohoku regions given by KAKUTA[13].

Origin time t_0 can be obtained by the three-parameter technique (e.g.,

JAMES et al.[14]) which is expressed by the equation

$$t_0 = t_p - \{1/(V_p/V_s - 1)\} \times t_{s-p} \tag{12}$$

where t_p=arrival time of P wave
t_{s-p}=S-P travel time
V_p=P wave velocity
V_s=S wave velocity

Since t_0 is computed for each station, the average of all the origin times computed is taken as the actual origin time.

Procedure of determining hypocenters on giving the actual origin time consists of three steps: The first step is to derive P-wave travel times T, from which a provisional hypocenter location is calculated for the homogeneous mantle structure with a velocity of 8.1 km/sec. The second step is to calculate travel time differences, δt, for all stations between travel times, T for the homogeneous mantle and T' for the mantle structure with two velocities obtained from the provisional hypocenter. Definition of these travel times is illustrated also in Fig. 11. The third step is to obtain a new set of travel times T' which is given by $T'=T+\delta t$. From the travel times T' the next provisional hypocenter is obtained. This procedure is iterated until the discrepancies are reduced to small values. In practice, the discrepancies were reduced with a few times of the iteration to a sufficiently small value. Figure 12 shows the travel times T and T', and travel time differences δt with respect to hypocentral depths. Even when the provisional hypocenter was deeper than the Moho boundary, we practically used these station corrections δt.

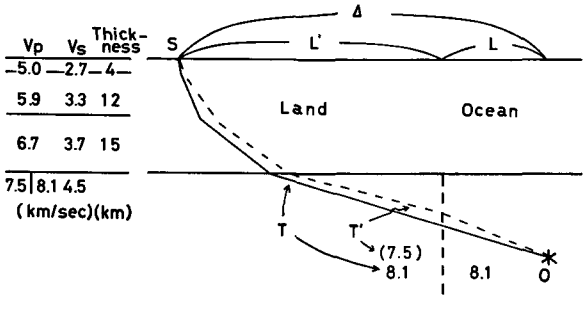

Fig. 11 Velocity distribution model applied to the hypocenter calculations and ray paths. A dashed line and a solid line from O to S represent the ray path in the three dimensional structure for the present analysis and that in the two dimensional structure from a hypocenter to a station, respectively.

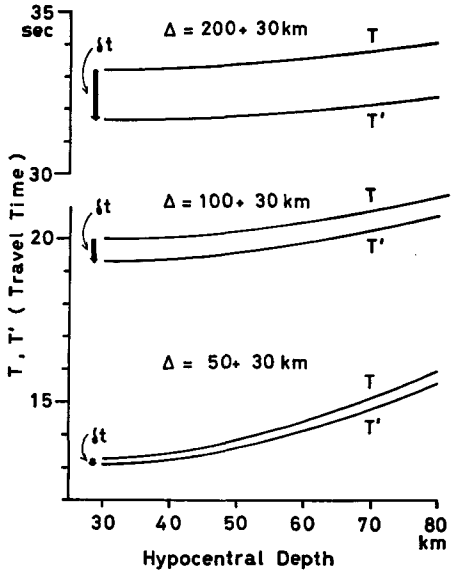

Fig. 12 Comparison of travel times for the three dimensional structure (T) and the two dimensional structure (T') which are shown in Figure 11.

3.2 Test of instability

The difference in network of stations as well as the difference in travel time tables affects hypocenter solution. Figure 13 shows the hypocenter locations of the 1973 Nemuro-Oki earthquake and its aftershocks which were determined by various method. Symbols attached to the epicenters are referred to in Table 4. The epicenters with symbol P were located by the present method. The epicenters with symbols P, 1, 2, and 3 were obtained by the three-parameter technique. The epicenters located by JMA are located in the southern limb of the region with scattering epicenters for the same earthquake, while the epicenters located by USGS are located in the northern limb of that region. The epicenter obtained when the low Pn-velocity model (models 1, 2, and 4 in Table 4) is used, is located more west than that obtained when the high Pn velocity model (model 3 in Table 4) is used.

The present epicenter locations were redetermined by using a small local network, while the ISC epicenters were located by using world wide network. However, discrepancies of the ISC epicenters from the relocated ones (symbol P) are small, that is, less than 10 km.

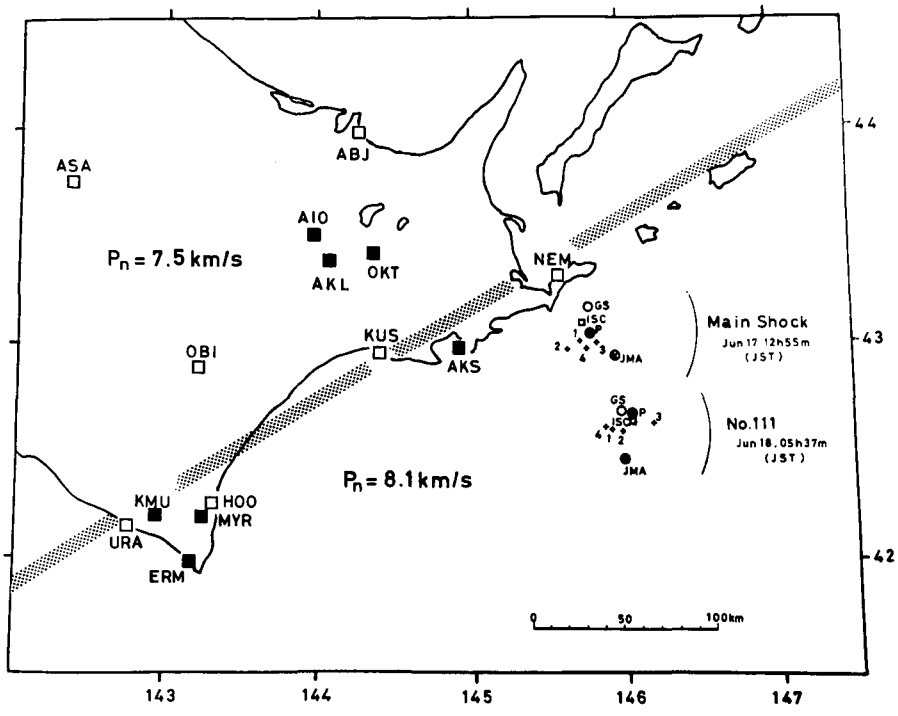

Fig. 13 Seismometric stations and two sets of epicenter solutions by different methods. Symbols attached to the epicenter see in Table 4. An open and a solid square represent the JMA station and the Hokkaido University station, respectively. Dotted belt represents a boundary between a high and a low *Pn* velocity zone in the laterally heterogeneous model applied for the hypocenter determination.

Table 4. Hypocenter solutions determined by different methods (see Fig. 13)

Notation	Network	Model	Main shock June 17, 03h55m		No. 111 June 17, 20h 37m	
			Depth (km)	Origin time GMT, (sec)	Depth (km)	Origin time GMT, (sec)
P	Fig. 13	*Pn*=7.5&8.1*	36	4.3		56.7
JMA	JMA Data	I-M	40	1.8	40	54.6
GS	USGS Data	J-B	48	2.9	50	57.3
ISC	ISC Data	J-B	41	1.9	10	52.0
1	JMA in Fig. 13	*Pn*=7.5*	34	4.2	20	56.2
2	Fig. 13	*Pn*=7.5*	30	4.2	27	56.1
3	Fig. 13	*Pn*=8.1*	27	4.2		56.1
4	Fig. 13	I-M	39	3.4	31	56.9

*: Crustal structure is shown in Fig. 11

3.3 Hypocenters of large earthquakes around Hokkaido

We have ten large earthquakes with $M=6.7$ or larger that occurred around Hokkaido (from 143°E to 148°E) during the period of 1952 to 1975 (Table 5). The epicenter locations of these earthquakes determined by the present method are shown in Fig. 14. The hypocenters located by JMA (CMO) and ISC (ISS) are also shown for comparison. The six earthquakes in the area from 145°E to 147°E have systematic difference in the locations of epicenters. The relocated epicenters differ by about 15 km from those by ISC (ISS), and the JMA epicenters are shifted from the ISC epicenters by 30 to 50 km toward the oceanic side. These discrepancies of epicenters are caused by the lateral variation in the uppermost part of the mantle. Since the CMO and ISS hypocenters of the 1952 Tokachi-Oki earthquake (No. 1 in Fig. 14) and its largest aftershock (No. 2) were determined by making no use of computer, the satisfied accuracy was not warranted in the hypocenters. The 1970 Hidaka earthquake (No. 7) occurred within the JMA network. The JMA and relocated epicenters for the earthquake were obtained at much

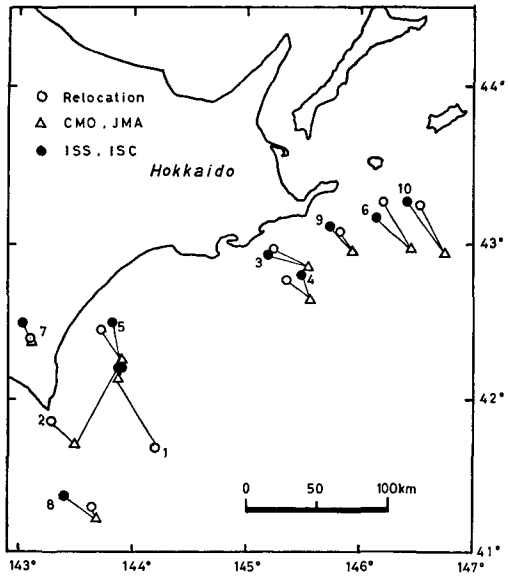

Fig. 14 Comparison of epicenters located by different methods. All earthquakes of $M=6.7$ or larger from 1952 to 1975 are shown. Located data are listed in Table 5.

the same place. In the later section, it will be given that the JMA and relocated epicenter may be more accurate than the ISC epicenters.

i) The 1973 Nemuro-Oki earthquake

The main shock of the 1973 Nemuro-Oki earthquake series occurred south off the Nemuro peninsula on June 17, 1973. The magnitude of this shock is 7.4. The eastern part of Hokkaido, particularly the area near the Nemuro peninsula, has been subject to extensive land subsidence for the past several decades[15]. A large seismic gap off eastern Hokkaido, where the earthquake occurred, has been pointed out by UTSU[16]. The Coordinating Committee for Earthquake Prediction has designated this area as "Special Observation Area" before the occurrence of this earthquake.

The relocated epicenters of the $M=4$ or larger aftershocks are shown in Fig. 15. The epicenters obtained by JMA and USGS are also shown in Figs. 16 and 17 for comparison. The aftershock region obtained from JMA epicenters is located about 30 km south of the relocated aftershock region. The existence of "aftershock swarm" on the northwestern side of the aftershock region is clearly identified in Fig. 15a. The aftershock swarm is also identified in Fig. 16, while that is hardly identified in Fig. 17.

Figure 18 shows S-P distribution of the aftershocks observed at AKS. High distribution of S-$P=4$ to 8 sec indicates the existence of the aftershock swarm. Scatter of the USGS epicenters may be associated with the fact that station sets for the determination of the USGS epicenters depend on the magnitude of earthquake.

Figure 15 shows that the aftershock region increased from 90 km$\times$90 km during the first day of the aftershock sequence to 120 km$\times$120 km before the largest aftershock of June 24. The largest aftershock of $M=7.2$ also has the other aftershock region near the east limb of the aftershock region of the main shock. The seismicity near the hypocenter of the main shock is low and the large aftershocks with $M=5$ or larger are mainly limited near the side of the trench.

Figure 19 shows the projection of the hypocenters with depth error less than 10 km in Fig. 15 onto the vertical cross-section along g-h in Fig. 1 which passes through Nemuro city and is almost perpendicular to the trench axis. The depth of the main shock is estimated to be 35 ± 5 km, which is shallower than the depth located by USGS, 48 km, and nearly the same as that by JMA, 40 km, or as that by ISC, 41 km.

In determining focal depths of aftershocks near the trench, a part of ISC

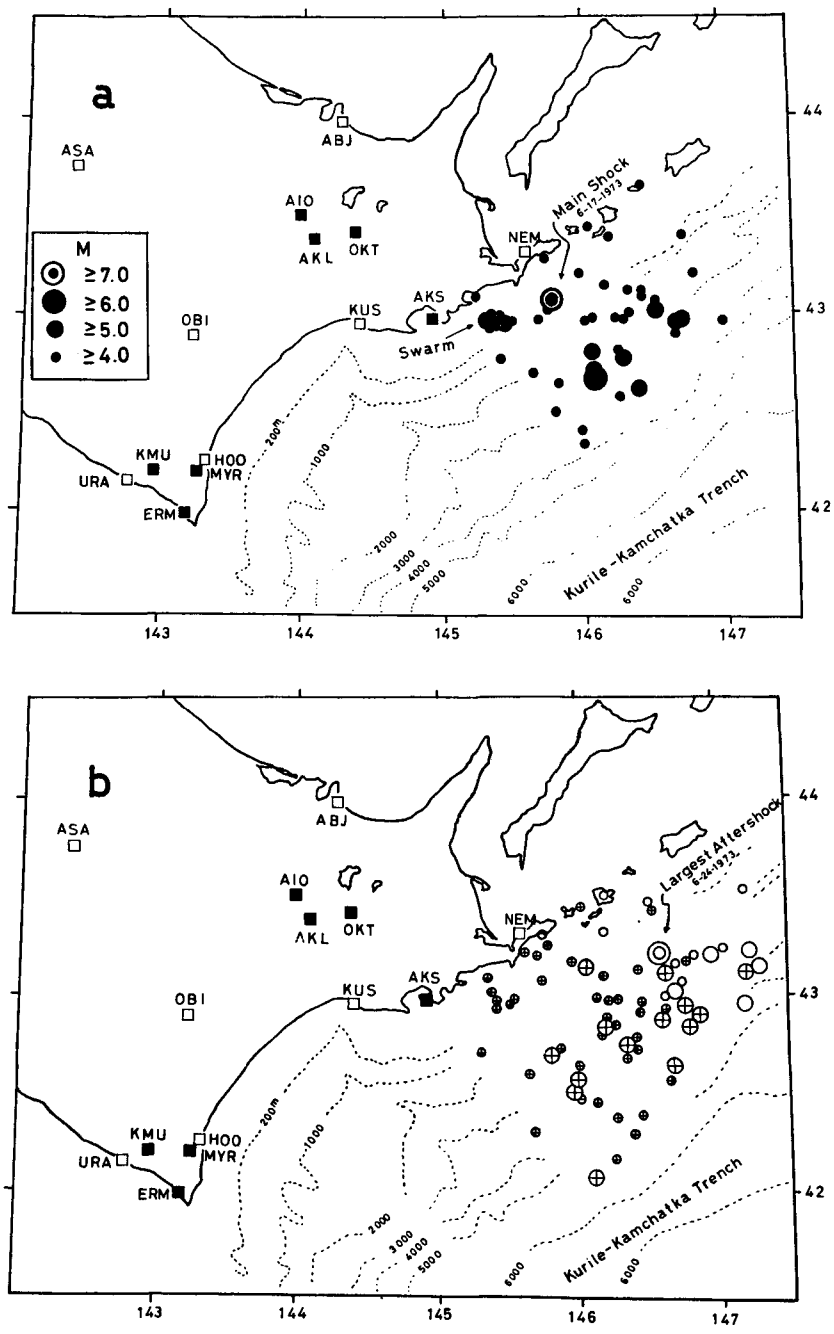

Fig. 15 Epicenters of the main shock and aftershocks of the 1973 Nemuro-Oki earthquake series located by the author. (a) A solid circle represents an event during the first day of the aftershock sequence. (b) A circle with a cross and an open circle represent an event after the first day to the largest aftershock of June 24 and an event after the largest aftershock to June 30, respectively.

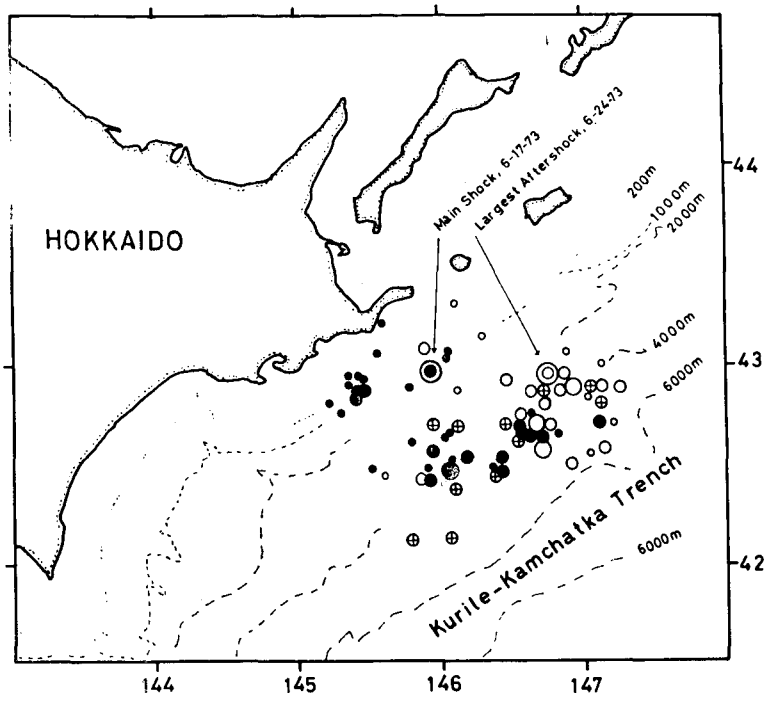

Fig. 16 Epicenters of the aftershocks located by JMA. Symbols of epicenters are the same as in Figure 15.

data was used. The focal depths for most of the aftershocks are shallower than the focal depth for the main shock. Hypocenters of large aftershocks in vicinity of the southern limb of the aftershock zone are shallower than those on the land side. Distribution of the hypocenters of the aftershocks except for the aftershock swarm seems to show a surface of the fault that is related to a tectonic motion of the main shock. The fault surface has a dip angle of about 24°. SHIMAZAKI[17] pointed out that the fault associated with this earthquake is a thrust type with low dip angle. The fault plane parameters he obtained are as follows: dip direction is N40°W and dip angle is 27°. The aftershock swarm also seems to show a nearly vertical fault associated with the secondary rupture following after the main thrust.

ii) The 1952 Tokachi-Oki earthquake

The main shock of the 1952 Tokachi-Oki earthquake (M=8.1) series occurred on March 4, 1952, off the Tokachi region, Hokkaido. The after-

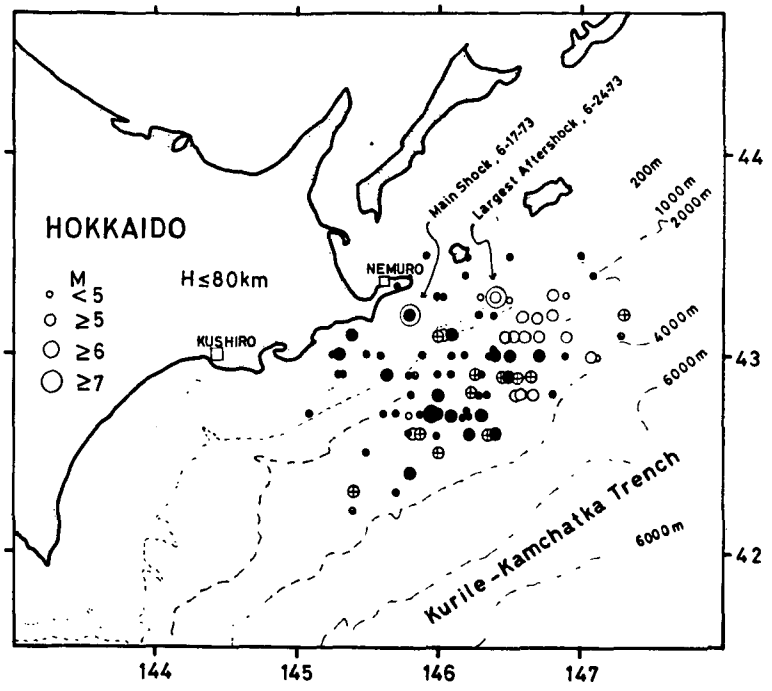

Fig. 17 Epicenters of the aftershocks located by USGS. Symbols of epicenters are the same as in Figure 15.

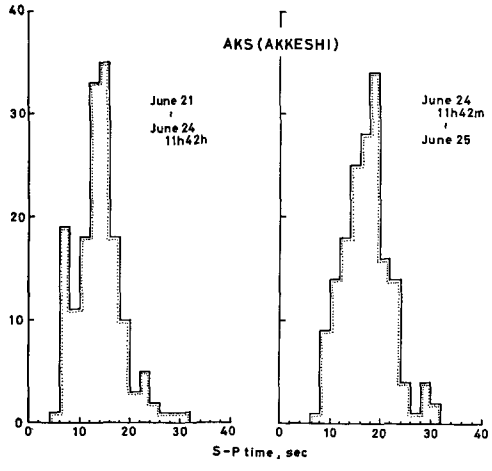

Fig. 18 *S-P* time distributions of the 1973 Nemuro-Oki earthquake series observed at Akkeshi (AKS).

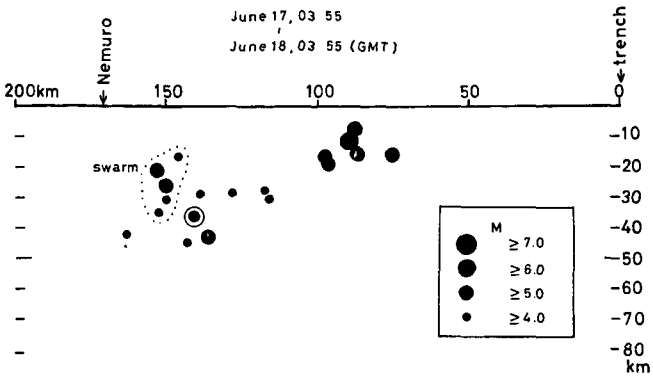

Fig. 19 Projection of hypocenters from Figure 15a onto the vertical cross-section *g-h* in Figure 1.

shock region was obtained by CMO (the Central Meteorological Observatory) and the tsunami source area was obtained by SUZUKI and NAKAMURA[18]. Dimension of the aftershock region as well as that of the tsunami source area is considerably small as compared with the standard dimension of the earthquake with the same magnitude. Recently HATORI[19] reexamined the tsunami source area and obtained its dimension as being four times as large as that obtained by SUZUKI and NAKAMURA. After the 1973 Nemuro-Oki earthquake occurred, ABE and YOKOYAMA[20] and HATORI[21),22] pointed out that a seismic gap between the 1952 earthquake and the 1973 earthquake still remains. On the other hand, SEKIYA et al.[23] relocated the epicenters of the Tokachi-Oki and the Nemuro-Oki earthquake series using the JMA standard travel-time tables and concluded that the seismic gap had already been reduced.

We redetermined here the locations of these epicenters with our method presented in Section 3.1. For the redetermination, 13 stations of CMO were used (Fig. 20). The relocated epicenters of the $M=5$ or larger aftershocks are shown in Fig. 21 in which the epicentral locations of the $M=5$ or larger aftershocks of the Nemuro-Oki earthquake are also shown. The western limb of the aftershock region is close to a line of the extension of the Hidaka mountain range. The eastern limb extends to about 60 km east of Kushiro sea canyon. As shown in the figure, little seismic gap between the Tokachi-Oki and the Nemuro-Oki earthquake exists. However, another large seismic gap between the main shock and the eastern swarm of the aftershocks is found, while the epicenters of small aftershocks located by SEKIYA et al.[23] fill

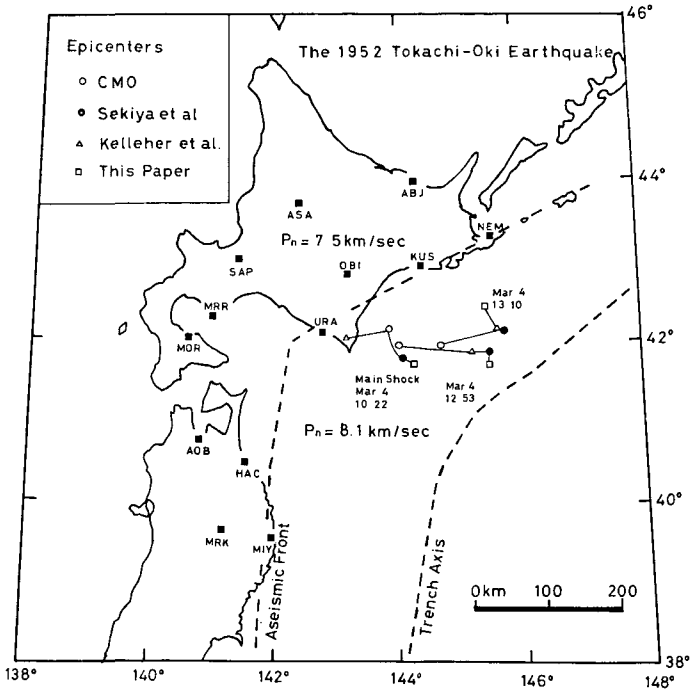

Fig. 20 Seismometric stations used for epicentral relocations. Three sets of epicenter solutions by different methods[23),33)] are shown. Aseismic Front represents a boundary between a high and a low *Pn* velocity zone in the laterally heterogeneous model applied for the epicentral determination.

this seismic gap, which seems to be apparent one. An additional point for the Tokachi-Oki and the Nemuro-Oki earthquake is that both earthquakes are the same in relatively low seismicity near the main shock.

Figure 20 shows the epicentral locations of the main shock of the 1952 Tokachi-Oki earthquake and its two large aftershocks determined by various methods. The differences between the epicentral locations determined by CMO and the present method are surprisingly large for all the shocks. For example, the CMO epicenters of an aftershock occurring at 12 h 53 m, March 4 is located 130 km west from the relocated epicenter. A dashed curve in Fig. 21a represents as aftershock region obtained from the CMO epicenters. This aftershock region is half or less as large as the relocated aftershock region. This large discrepancy may strongly depend on method of hypocentral determination. The lateral variation of the upper mantle velocity may hardly affect this discrepancy. This is apparent in the fact that the average

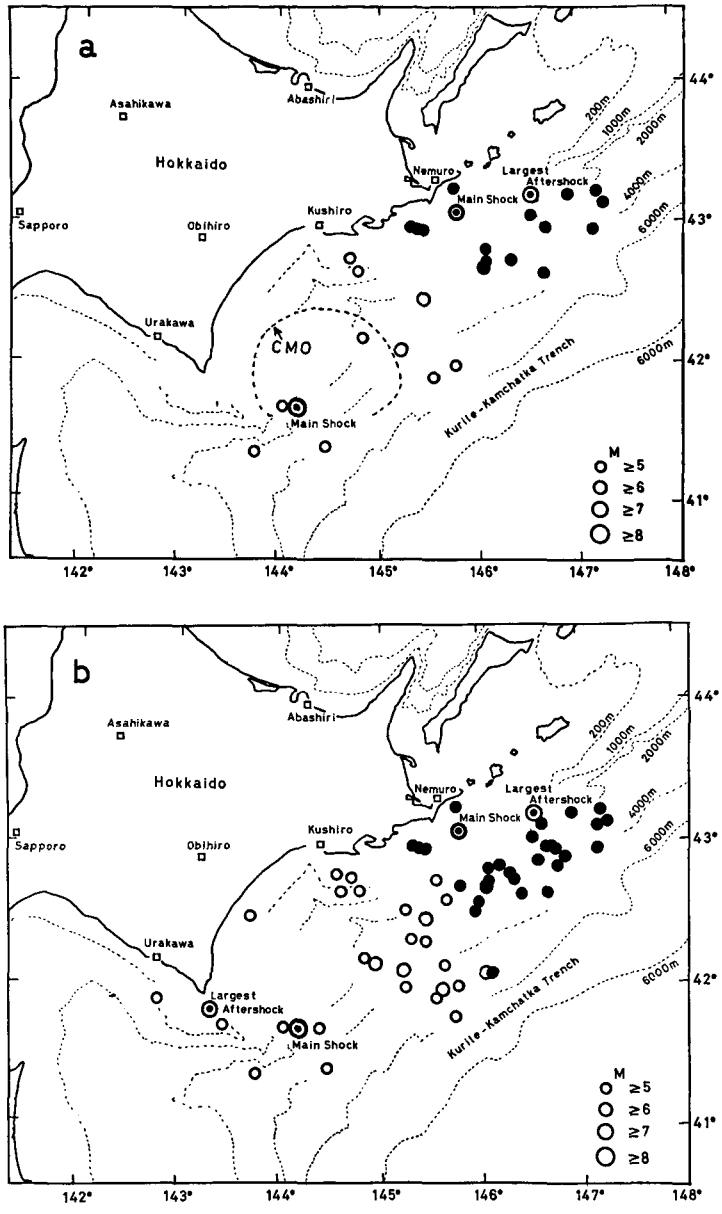

Fig. 21 Relocated epicenters of the $M=5$ or larger aftershocks of the 1952 Tokachi-Oki earthquake (open circles). Epicenters of the 1973 Nemuro-Oki earthquake series are also shown (solid circles). Upper: events during the first day of the aftershock sequence. An enclosed curve represents the aftershock zone of the Tokachi-Oki earthquake on the basis of the CMO epicenters. Lower: events during the first ten days of the aftershock sequence.

difference between the relocated epicenters determined by taking the lateral variation of the velocity into account and the epicenters determined by taking no lateral variation of the velocity into account is about 10 km, which is very small compared with that for the 1973 Nemuro-Oki earthquake series.

iii) The Akkeshi-Oki earthquake

The main shock of the 1961 Akkeshi-Oki earthquake occurred on August 11, 1961, (GMT), off Akkeshi, Hokkaido. JMA assigned the main shock parameters as follows; location is 42°51'N and 145°34'E, origin time is 15 h 51 m 31.9 sec (GMT); focal depth is 80 km; and M=7.2. The KUS station located in Kushiro city observed 54 aftershocks during the first 10 days after the main shock. Applying the present method of hypocenter determination to these shocks, we relocated the hypocenters of the main shock and aftershocks during the first 10 days after the main shock (Fig. 22). Figure 23 show a projection of the hypocenters onto the vertical cross-section along A-A' line in Fig. 22 that is approximately perpendicular to the trench axis. The aftershock region with a horizontal length of 30 or 40 km is located in a depth range from 35 to 50 km. The relocated parameters are assigned as follows: location is 42.98°N and 145.25°E, and focal depth is 36 km.

ABE (unpublished data) showed that the fault associated with this earthquake is a thrust type. The fault plane parameters he obtained are

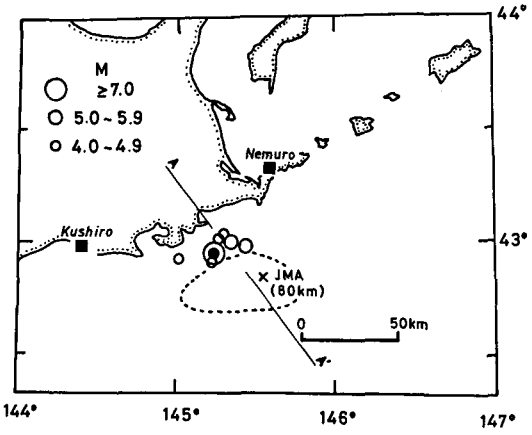

Fig. 22 Epicentral locations of the 1961 Akkeshi-Oki earthquake (double circle) and aftershocks (open circles) through August 31, 1961. An enclosed curve represents the aftershock zone on the basis of the JMA epicenters.

as follows: dip direction is N35°W, dip angle is 24°. The dip angle is much the same as that of the 1973 Nemuro-Oki earthquake. An additional point for the present earthquake is that a depth of the Moho boundary off Tokachi determined from seismic and gravitational data is 30 to 35 km according to the work of SATO[24]. From these results, it may be concluded that a main rupture of this earthquake occurred just beneath the Moho boundary and no rupture extends into the crust.

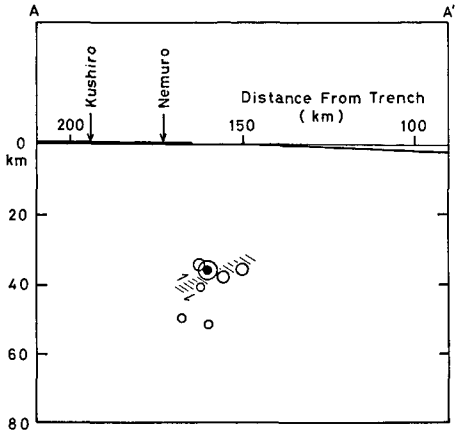

Fig. 23 Projection of hypocenters from Figure 22 onto the vertical cross-section A-A'. Hached belt represents an assumed fault surface.

iv) The 1970 Hidaka earthquake

The main shock of the 1970 Hidaka earthquake occurred on January 20, 1970, (GMT), under the southern part of the Hidaka mountains. JMA assignes the main shock parameters as follows: location is 42°23'N and 143° 08'E; origin time is 17h 33 m 03.8 sec (GMT); focal depth is 50 km; and M= 6.7. JMA reported the eight aftershocks (M=3.9 to 4.8) taking place in January, 1970. We relocated the hypocenter locations of six large aftershocks among these as shown in Fig. 24 using data of several stations including four stations of KMU, HOO, URA, and OBI. Figure 24 also shows the epicenter of the main shock located by JMA which is very close to the relocated one, while the epicenters by USCGS and ISC are 15 km northwest of the relocated epicenter. The epicenters of small aftershocks, which were located by MORIYA[25] using small network of temporary stations, are distributed in and around the relocated aftershock region. Therefore, it may safely be concluded

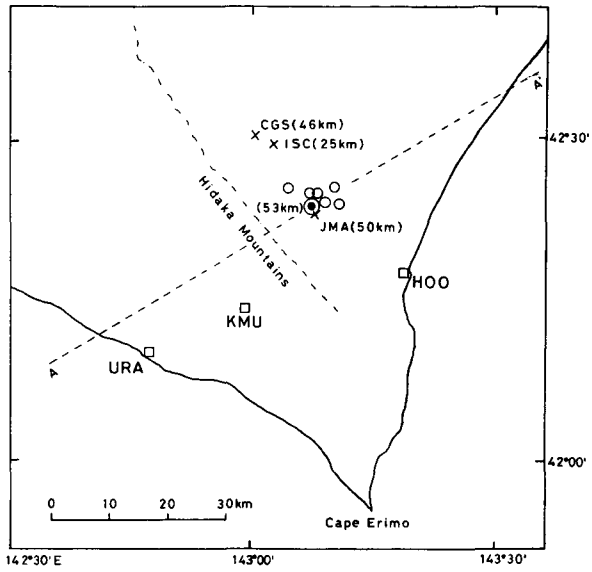

Fig. 24 Epicentral locations of the 1970 Hidaka earthquake (double circle) and aftershocks (open circles) through January 31, 1970.

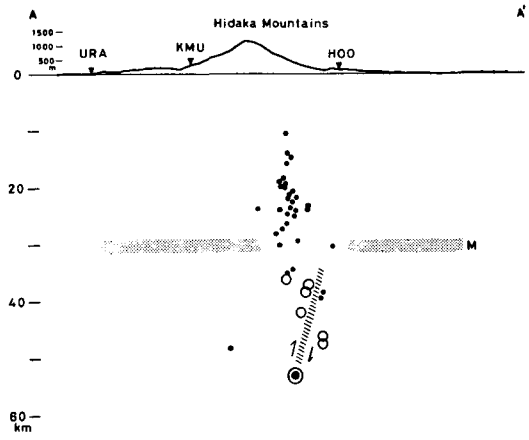

Fig. 25 Projection of hypocenters from Figure 24 onto the vertical cross-section A-A'. A double and six open circles represent the main shock and large aftershocks, respectively. Small solid circles represent the small aftershocks of $M=3.5$ or smaller located by MORIYA[25]. A hatched belt represents an assumed fault surface.

that the epicenters located by us and JMA for the main shock are more accurate than those by USCGS and ISC.

Figure 25 shows a projection of hypocenters onto the vertical cross-section along A-A' line in Fig. 24. The main shock and the six large aftershocks (M=3.9 to 4.5) are distributed in depths from 35 to 53 km, while small aftershocks are almost distributed in depths from 15 to 30 km. The distribution of these hypocenters is also confirmed in S-P time distribution for the main shock and its aftershocks obtained at KMU and HOO. Figure 26 shows the S-P time distribution at both stations KMU and HOO. The S-P time distribution of KMU may be separated into two groups at a S-P time of 4.8 sec. The same separation is also possible in the S-P distribution at HOO. S-P times of the main shock and the large aftershocks are distributed in times from 4.8 to 6.0 sec, while the S-P times of all shocks are distributed in times from 3.4 to 6.4 sec. If epicentral distances from all shocks to station HOO are nearly the same each other, these large S-P times of the main and aftershocks correspond to deeper locations of focal depths in the aftershock zone.

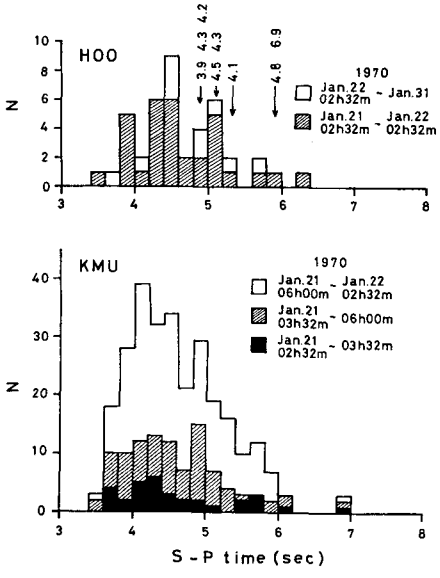

Fig. 26 S-P time distributions of the 1970 Hidaka earthquake series observed at Hiroo (HOO) and Kamikineusu (KMU). Numbers attached to arrows in the upper part of figure indicate magnitudes of the mainshock and seven large aftershocks.

YOSHII[26] estimated a depth of the Moho boundary under the Hidaka region to be in a range from 30 to 35 km from seismic and gravitational data. In Fig. 25, the Moho boundary is roughly shown. A S-P time of 4.8 sec is to be given by an earthquake with a depth near the Moho boundary. The fault plane parameters obtained by SASATANI (unpublished data) for the earthquake are as follows: dip direction is S77°W and dip angle is 76°. The hypocenter distribution of the large aftershocks seems to show a main thrust and nearly vertical fault which may be related to a tectonic motion of the main shock (see Fig. 25). The main rupture for the main shock might be inferred as being started from the bottom of fault area and being propagated upward to the Moho boundary. Existence of many small aftershocks over the Moho boundary suggests that the secondary cracks are triggered by the main rupture in the lower crust.

4. Discussion of results

We have shown lateral variation of P-wave velocity in the upper mantle and distribution of the hypocenters of large earthquakes and their aftershocks which are relocated in consideration of heterogeneity of the upper mantle in northern Japan. A schematic representation of the vertical section along *e-f* line in Fig. 1 which is almost perpendicular to the trench axis is shown in the lower part of Fig. 27, in which the obtained velocity distribution in the upper mantle is summarized. In this figure, the works on the seismicity by UMINO and HASEGAWA[27] and Tohoku University[28] are referred to.

Since the good agreement of the high velocity zone with the high seismicity zone was obtained in the uppermost mantle considered in this area, it may be possible to assume that the same agreement will be available in the deep seismic zone. The existence of the dipping high-V zone may mainly produce large scatter of travel-time plots as shown in Figs. 3c and 3d. For example, if waves from the hypocenter of the Izu-Hanto earthquake to the stations located near the Sea of Japan travel not in the dipping high-V zone, but in the low-V zone of 7.5 to 7.7 km/sec, then the arrivals of the waves will be later at the stations; if waves from the same hypocenter to the stations located near the Pacific Ocean travel in both high-V and low-V zones, then the arrivals of the waves will be earlier at the stations.

Hypocenters of earthquakes in and around Hokkaido were relocated because of the existence of the lateral variation of the upper mantle velocity. An upper mantle model used for hypocenter determination was given on the basis of the results in Chapter **2**. Aftershock hypoctenters of the large

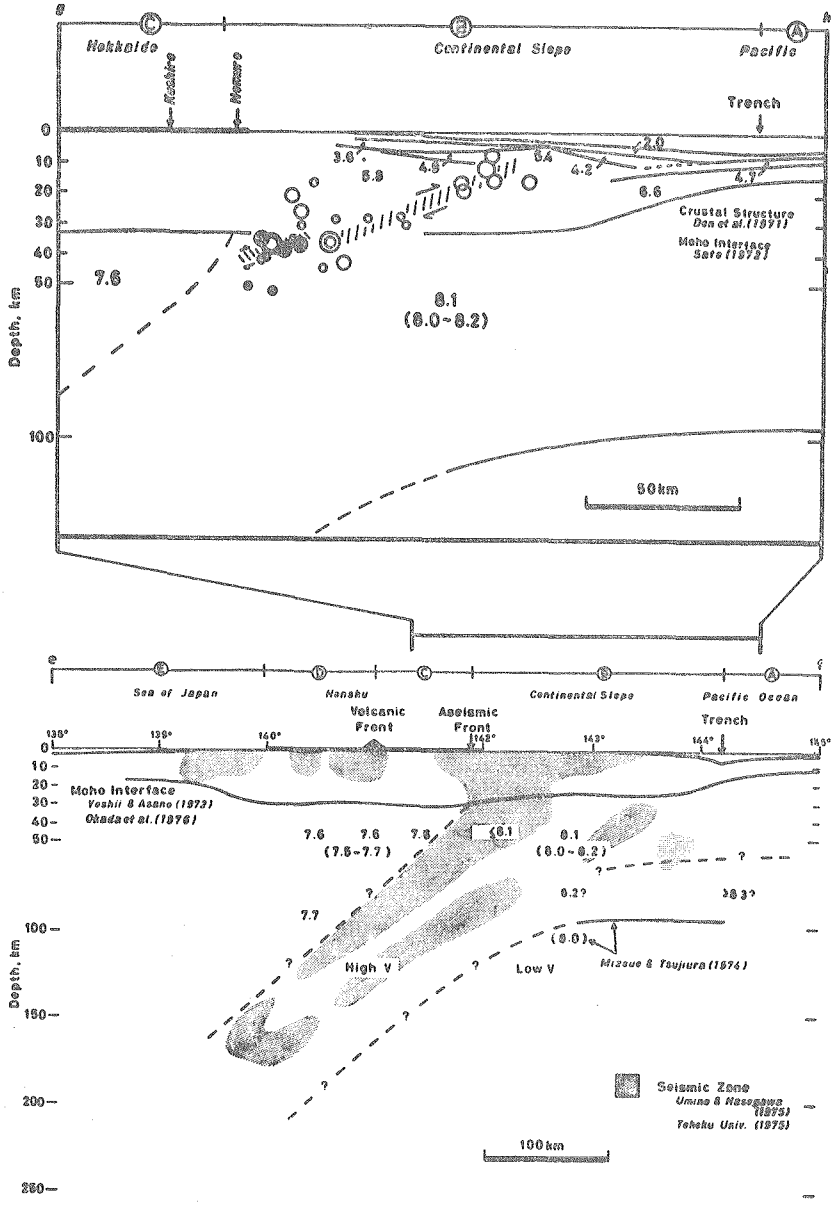

Fig. 27 Schematic representation of the deep structure[9),12),24),34)] and seismic activity[27),28)] in Northern Japan. Upper: projection of hypocenters of the 1961 Akkeshi-Oki earthquake series (solid circles) and the 1973 Nemuro-Oki earthquake series (open circles) onto the vertical cross-section *g-h* in Figure 1. Lower; *P*-wave velocity (in km/sec) in the upper mantle and representative cross section beneath the northern part of the Japanese island arc along the *e-f* line shown in Figure 1.

Table 5. Hypocentral data of earthquakes larger than $M=6.7$ in and around Hokkaido for the period 1952–1975 (see Fig. 28)

Earthquake No.	Data	Date and Time (GMT)	Origin Time	Epicenter	Depth	M	m*
1	Relocation	1952 Mar. $04^{d}01^{h}$	$22^{m}43.6^{s}$	41.69°N 144.22°E	35**		
	CMO			42.15 143.87	45	8.1	2.5
	ISS		22 40.	42.2 143.9			
2	Relocation	1952 Mar. 09 17	03 52.7	41.86 143.3	48		
	CMO			41.7 143.5	0-20	7.0	−1
	ISS		03 12.	42.2 143.9			
3	Relocation	1961 Aug. 11 15	51 37.1	42.98 145.25	36		
	JMA		51 31.9	42.85 145.57	80	7.2	−1
	ISS		51 34	42.94 145.21	37		
4	Relocation	1961 Nov. 15 07	17 13.8	42.78 145.38	35**		
	JMA		17 09.9	42.65 145.57	60	6.9	−1
	ISS		17 06.	42.79 145.5	00		
5	Relocation	1962 Apr. 23 05	58 12.6	42.42 143.81	80		
	JMA		58 11.8	42.23 143.92	60	6.9	−1
	ISS		58 12.	42.45 143.83	66		
6	Relocation	1964 Jun. 23 01	26 39.8	43.27 146.22	62		
	JMA		26 34.9	42.98 146.47	80	7.1	
	ISC		26 36.8	43.16 146.17	76	6.4	
7	Relocation	1970 Jan. 20 11	02 04.1	42.40 143.13	53		
	JMA		02 03.8	42.38 143.13	50	6.7	
	ISC		02 03.1	42.48 143.04	25	6.3	
8	Relocation	1971 Aug. 02 07	24 57.5	41.29 143.65	53		
	JMA		24 55.1	41.23 143.07	60	7.0	−0.5
	ISS		24 56.0	41.37 143.44	45	6.5	
9	Relocation	1973 Jun. 17 03	55 04.3	43.09 145.83	36		
	JMA		55 01.8	42.97 145.95	40	7.4	1.5
	ISC		55 01.9	43.12 145.74	41	6.5	
10	Relocation	1973 Jun. 24 02	43 25.6	43.23 145.56	35**		
	JMA		43 21.9	42.95 146.75	30	7.1	0.5
	ISC		43 22.8	43.29 146.43	26	6.3	

*: Tsunami magnitude which was given by Hatori[21].
**: Tentatively restrained.

earthquakes were also relocated, from which aftershock zones to be related to fault planes of the main shock were obtained. Figure 28 shows the aftershock zones of the large earthquakes (Table 5) from Hokkaido to the southern Kurile islands to which the results in Chapter **3** and those from ISC data were

supplied. Large and small symbols represent the main shocks and the aftershocks of $M=5$ or larger, respectively. This figure gives evidence that little or no seismic gap exists in the region as shown in this figure so that a large earthquake of $M=7.5$ or more is not anticipated in this region in the near future.

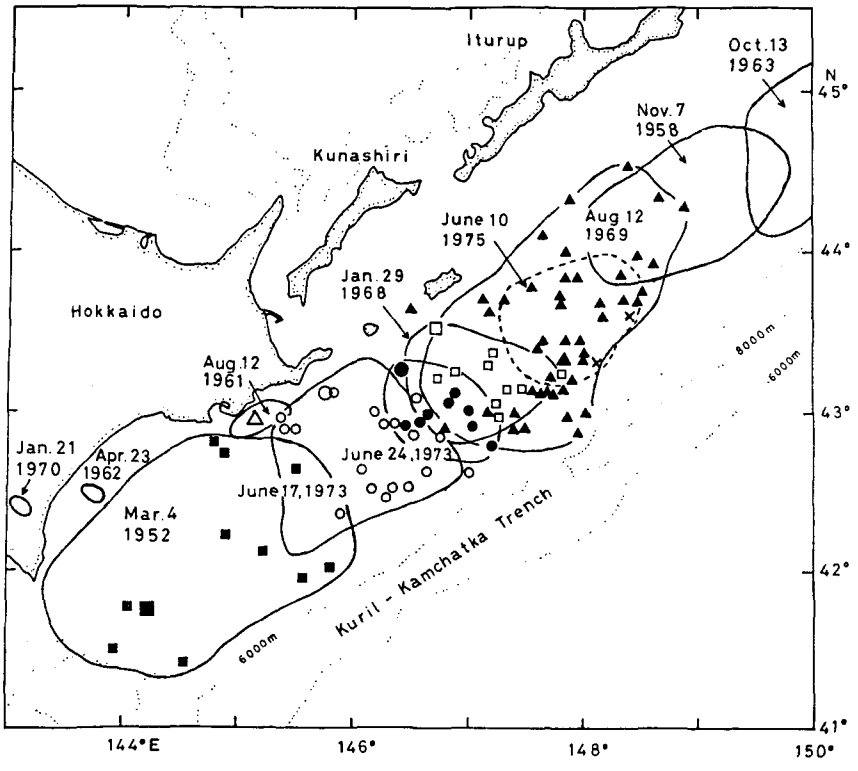

Fig. 28 Aftershock regions of large earthquakes of $M=6.7$ or larger during the period of 1952 to 1975. Epicenters and aftershock regions of the 1968, 1969, and 1973 earthquakes are obtained from the ISC data. Large and small symbols indicate epicenters of the main shocks and aftershocks of $M=5$ or larger, respectively.

We obtained vertical sections of aftershocks for the Nemuro-Oki, the Akkeshi-Oki, and the Hidaka earthquake. The upper part of Fig. 27 shows projection of aftershock zones of the Nemuro-Oki and the Akkeshi-Oki earthquake onto the vertical section along *g-h* line in Fig. 1. Crustal structures and the Moho interface are referred to from the explosion seismic

study of DEN et al.[12] and the gravitational study of SATO[24] for the region off Tokachi. The significance of tectonic features is that most of the aftershocks of the Nemuro-Oki earthquake are distributed within the continental thick crust beneath a region of the continental slope is the Pacific Ocean. From the facts analysed, it may be concluded that the seismic energy of this large thrust-type earthquake was accumulated mostly within the thick crust, and the main thrust rupture started from the uppermost part of the mantle on the coastal side and came up to just under the sea bottom near the trench.

Based on the features, it may be inferred that the surface of fault is a part of the boundary diving the continental crust of Hokkaido from the dipping oceanic plate. Since a dip angle of the fault surface is 24°, the boundary to be extended to the trench, therefore, must be curved with upward convex.

The Akkeshi-Oki earthquake has nearly the same focal solution as that of the Nemuro-Oki earthquake. The analysis of this earthquake shows that its main rupture occurred at the top of the mantle and did not extend into the crust.

5. Conclusions

The following results may be drawn from the present study.

(1) *Pn* velocity under the region on the land side of the Aseismic Front is 7.5 to 7.7 km/sec which is lower than that of the Pacific Ocean. *Pn* velocity under the volcanic region may be little lower than that under the non-volcanic region in the island. Based on the results as well as travel times in these regions, a model of the crust and upper mantle structure under the island of northern Japan was derived which is referred to as the Northern Japan model.

(2) *Pn* velocity in the seismic region from the trench to Aseismic Front is more than 8.0 km/sec which is higher than that in a region on the land side. As an upper mantle structure in the seismic region the Pacific Coast model may be proposed in which *Pn* velocity is taken as 8.1 km/sec and velocity gradient with depth is assumed as being more gentle than that in the *J-B* model.

(3) Velocity of the upper mantle laterally varies from 8.0 km/sec near the coast to 8.3 km/sec near the trench in the Pacific Ocean. This may be referred to as the lateral variation of the velocity. However, this lateral variation of the velocity could be interpreted as apparent one.

(4) The lateral variation of the upper mantle velocity causes systematic error in epicenter location of earthquakes occurring in the Pacific coast. The

relocated epicenters determined by taking the lateral variation of the velocity into account have higher reliabilities than the epicenters determined by taking no lateral variation of the velocity into account.

(5) Little seismic gap exists in the Pacific coastal area east of Hokkaido so that a large earthquake of $M=7.5$ or more is not anticipated in this region in the near future.

(6) Aftershock region of the 1973 Nemuro-Oki earthquake increased from 90 km×90 km during the first day of the aftershock sequence to 120 km× 120 km before the largest aftershock of June 24. The main thrust rupture of this earthquake started from the uppermost part of the mantle and came up to just under the sea bottom near the trench.

Acknowledgements. I am much indebted to the staffs of Japan Meteorological Agency, Tohoku University, University of Tokyo, and Hokkaido University for suppling their data from seismic stations for this study. The field observations were greatly assisted by Mr. Muneo Okayama. The focal mechanism solutions of section 3.3 were taken by Dr. Katsuyuki Abe and Mr. Tsutomu Sasatani. The original programs for computing hypocenters and travel times were taken by Drs. Kazuo Shibuya, Kiyoshi Ito, and Hiromu Okada. I am much indebted to Prof. Hiroshi Okada for critical reading of the manuscript and for offering many valuable suggestions. I am also thank Prof. Kyozi Tazime and the members of the Research Center for Earthquake Prediction, Hokkaido University for their encouragement during this study.

Numerical computations were carried out by FACOM 230–75 at the Hokkaido University Computing Center.

This paper was submitted to the Hokkaido University in March, 1977 as the author's doctorial thesis.

References

1) Utsu, T.: Seismological evidence for anomalous structure of island arcs with special reference to the Japanese region. Review Geophys. Space Phys., **9** (1971) 839–890.
2) Abe, K., M. Kishio, and N. Yamakawa: Precision and accuracy of hypocenters and origin times of earthquakes in and near the Japanese Islands (II), – The case of the Etorofu earthquake of 1963 and its aftershocks–. Zisin, **24** (1972) 335–343, (in Japanese).
3) Asano, S., H. Okada, T. Yoshii, K. Yamamoto, T. Hasegawa, K. Ito, S. Suzuki, A. Ikami, and K. Hamada: Crust and upper mantle structure beneath northeastern Japan as revealed from explosion seismic observations. J. Phys. Earth., (1978) (in preparation).
4) Okada, H., S. Asano, T. Yoshii, A. Ikami, S. Suzuki, T. Hasegawa, K. Yamamoto, K. Ito and K. Hamada: Regionality of the upper mantle around northeastern

Japan as revealed by big explosions at sea, SEIHA-1 explosion experiment. J. Phys. Earth., (1978) (in preparation).

5) YOSHII, T.: Proposal of the "Aseismic Front". Zisin, **28**, (1975) 365–367, (in Japanese).

6) SUZUKI, S.: Determination of earthquake hypocenters in consideration of the lateral variation of velocity in the upper mantle beneath the island arcs of Japan, On the Nemuro-Hanto-Oki earthquake of 1973. Zisin, **28** (1975) 181–199, (in Japanese).

7) UTSU, T.: Anomalous structure of the upper mantle beneath the Japanese islands, J. Fac. Sci., Hokkaido Univ., **25** (1971) 99–128, (in Japanese).

8) YAMAMIZU, F.: P travel time anomaly in Japan as deduced from three-dimensional seismic ray tracing. Geophy. Bull. Hokkaido Univ., **30** (1973) 33–56, (in Japanese).

9) MIZOUE, M., and M. TSUJIURA: Azimuthal variation of upper mantle structure from P-wave travel time residuals at Dodaira micro-earthquake observatory. Bull. Earthq. Res. Inst., **12** (1974) 57–71, (in Japanese).

1;) FEDOTOV, S.A. and L.B. SLAVINA: An estimate of the longitudinal wave velocities in the upper mantle under the northwestern part of the Pacific Ocean and Kamchatka. Izv. Earth Physics, (1968) 8–13.

11) ASADA, T and H. SHIMAMURA: Observation of earthquakes and explosions at the Bottom of the western Pacific: Structure of oceanic lithosphere revealed by longshot experiment. A.G.U. Monograph, **19** (1976) 135–153.

12) DEN, N., H. HOTTA, S. ASANO, T. YOSHII, N. SAKAJIRI, Y. ICHINOSE, M. MOTOYAMA, A.E. BERESNEV and A.A. SAGALEVITCH: Seismic refraction measurements around Hokkaido. Part 1. Crustal structure of the continental slope off Tokachi. J. Phys. Earth, **19** (1971) 329–345.

13) KAKUTA, T.: Regional features in the upper mantle, based on the relation between apparent Poisson's ratio and the mechanical structure. Rep. Fac. Sci., Kagoshima Univ., **2** (1969) 103–125.

14) JAMES, E.J., I.S. SACKS, E.L. LAZO, and P.G. APARICIO: On locating local earthquake using small netwarks. Bull. Seism. Soc. Amer., **59** (1969) 1201–1212.

15) Geographical Survey Institute: Vertical displacements in the eastern part of Hokkaido. Rep. of the Coordinating Committee for Earthquake Prediction, **5** (1971) 1–2.

16) UTSU, T.: Large earthquakes near Hokkaido and the expectancy of the occurrence of a large earthquake off Nemuro. Rep. of the Coordinating Committee for Earthquake Prediction, **7** (1972) 7–13 (in Japanese).

17) SHIMAZAKI, K.: Nemuro-Oki earthquake of June 17, 1973: A lithospheric rebound at the upper half of the interface, Phys. of the Earth and Planet. Interiors, **9** (1974) 314–327

18) SUZUKI, Z. and K. NAKAMURA; On the heights of the tsunami on March 4, 1952, in the district near Erimo-misaki. Sci. Rep. Tohoku Univ. Geophys., **4** (1953) 139–142.

19) HATORI, T. Reexamination of the wave source of the 1952 Tokachi-Oki tsunami. Zisin, **26** (1973). 206–208, (in Japanese).

20) ABE, K., and I. YOKOYAMA: An expected major earthquake off the coast of eastern Hokkaido. General Report on the Earthquake off the Nemuro Peninsula, June 17, 1973 (1974) 210–214, (in Japanese).

21) HATORI, T.: Source area of the tsunami off the Nemuro peninsula in 1973 and its comparison with the Tsunami in 1894. Bull. Earth. Res. Inst., **13** (1974) 67–76.

22) HATORI, T.: Tsunami activity in eastern Hokkaido after the Off Nemuro Peninsula earthquake in 1973. Zisin, **28** (1975) 461–471, (in Japanese).

23) SEKIYA, H., S. HISAMOTO, E. MOCHIZUKI, E. KOBAYASHI, T. KURIHARA, K.

TOKUNAGA and M. KISHIO: The off Nemuro peninsula earthquake of the large earthquakes off southern part of Hokkaido. Kenshinjiho, JMA, **39** (1974) 33–39, (in Japanese).

24) SATO, M.: The crustal section across the Tohoku district and the continental slope off Tokachi, Hokkaido, Geophy. Bull. Hokkaido Univ., **27** (1972) 25–40, (in Japanese).

25) MORIYA, T.: Aftershock activety of the Hidake mountains earthquake of January 21, 1970. Zisin, **24** (1972) 287–297, (in Japanese).

26) YOSHII, T.: Terrestrial heat flow and features of the upper mantle beneath the Pacific and the Sea of Japan, J. Phys. Earth, **20** (1972) 271–286.

27) UMINO, N. and A. HASEGAWA: On the two layered structure of deep seismic plane in northeastern Japan arc. Zisin, **28** (1975) 125–139, (in Japanese).

28) Tohoku University: Telemetering system for seismic observation. Coll. Abstr. Autumn Meet. Seismol. Soc. Jap., (1975), **23**, (in Japanese).

29) SUZUKI, S.: Aftershock region of the 1970 Hidaka earthquake. Coll. Abstr. Autumn Meet. Seismol. Soc. Jap., (1975), **16**, (in Japanese).

30) HASEGAWA, T., S. HORI, A. HASEGAWA, K. KASAHARA, S. HORIUCHI and J. KOYAMA: On the mechanisms of the earthquakes of southeastern part of Akita prefecture in 1970. Zisin, **27** (1974) 302–312, (in Japanese).

31) Reseach Group for Aftershocks: Observation of the main and aftershocks of the earthquake off the Izu Peninsula, 1974, Rep. of the Coordinating Committee for Earthquake Prediction, **13** (1975) 54–58, (in Japanese).

32) ICHIKAWA, M. and E. MOCHIZUKI: Travel time tables for local earthquaues in and near Japan. Papers in Meterology and Geophysics, **22** (1971) 229–290.

33) KELLEHER, J., L. SYKES, and J. OLIVER; Possible criteria for predicting earthquake locations and their application to major plate boundaries of the Pacific and the Caribbean. J.G.R., 78, **14** (1973) 2745–2585.

34) YOSHII, T. and S. ASANO: Time-term analyses of explosion seismic data. J. Phys. Earth, **20** (1972) 47–57.